Experimental Neurology 313 (2019) 60–78

Contents lists available at ScienceDirect

Experimental Neurology

journal homepage: www.elsevier.com/locate/yexnr

Research paper

Treadmill exercise ameliorates focal cerebral ischemia/reperfusion-induced neurological deficit by promoting dendritic modification and synaptic plasticity via upregulating caveolin-1/VEGF signaling pathways

Qingfeng Xie, Jingyan Cheng, Guoyuan Pan, Shamin Wu, Quan Hu, Haoming Jiang, Yangyang Wang, Jianrong Xiong, Qiongyi Pang, Xiang Chen*

Physical Medicine and Rehabilitation Center, The Second Affiliated Hospital and Yuying Children's Hospital of Wenzhou Medical University, No. 109, Xueyuanxi Road, Wenzhou 325027, Zhejiang, China

ARTICLE INFO

Keywords:
MCAO
Treadmill exercise
Caveolin-1/VEGF
Dendrite
Dendritic spine
Synaptic plasticity

ABSTRACT

Dendritic and synaptic plasticity in the penumbra are important processes and are considered to be therapeutic targets of ischemic stroke. Treadmill exercise is known to be a beneficial treatment following stroke. However, its effects and potential mechanism in promoting dendritic and synaptic plasticity remain unknown. We have previously demonstrated that the caveolin-1/VEGF signaling pathway plays a positive role in angiogenesis and neurogenesis. Here, we further investigated the effects of treadmill exercise on promoting dendritic and synaptic plasticity in the penumbra and whether they involve the caveolin-1/VEGF signaling pathway. A middle cerebral artery occlusion (MCAO) animal model was established, and rats were randomly divided into eleven groups. At 2 days after MCAO, rats were subjected to treadmill exercise for 7 or 28 days. Daidzein (a specific inhibitor of caveolin-1, 0.4 mg/kg) was used to confirm the effect of caveolin-1/VEGF signaling on exercise-mediated dendritic and synaptic plasticity. Neurobehavioral performance, tissue morphology and infarct volumes were detected by Modified Neurology Severity Score (mNSS), Hematoxylin-eosin (HE), and Nissl staining, while neural plasticity and its molecular mechanism were examined by Golgi-Cox staining, transmission electron microscopy, western blot analysis and immunofluorescence. We found that treadmill exercise promoted dendritic plasticity in the penumbra, consistent with the significant increase in caveolin-1 and VEGF expression; improved neurological recovery; and reduced infarct volume. In contrast to the positive effects of the treadmill, a caveolin-1 inhibitor abrogated the dendritic and synaptic plasticity. Furthermore, we observed that treadmill exercise-induced improved dendritic and synaptic plasticity were significantly inhibited by the caveolin-1 inhibitor, consistent with the lower expression of caveolin-1 and VEGF, as well as the worse neurobehavioral state. The findings indicate that treadmill exercise ameliorates focal cerebral ischemia/reperfusion-induced neurological deficit by promoting dendritic and synaptic plasticity via upregulating caveolin-1/VEGF signaling pathways.

1. Introduction

Ischemic stroke is caused by the blockage of an artery in the brain, accounting for approximately 87% of stroke cases, which contributes to the major portion of death and post-stroke disability in patients (Benjamin et al., 2018). There are at least three processes during recovery after stroke: resolution of acute tissue damage, behavioral compensation, and plasticity (Carmichael, 2003). Most studies focus on reducing oxidative stress, attenuating Ca2+ overload, inhibiting apoptosis, ameliorating microcirculation, enhancing neurogenesis, and cell differentiation in the acute stage. Recent studies have shown that dendritic and synaptic plasticity in the penumbra are important processes and are considered to be therapeutic targets of ischemic stroke in the recovery stage (Ito et al., 2006; Blizzard et al., 2011).

Abbreviations: MCAO, middle cerebral artery occlusion; VEGF, vascular endothelial growth factor; MAP-2, microtubule-associated protein-2; PSD, postsynaptic density; SYN I, synapsin I; S, sham-operated; M, model; SI, inhibitor treated shams; EM, treadmill exercise trained models; IM, inhibitor treated models; IEM, inhibitor treated and treadmill exercise trained models; bFGF, basic fibroblast growth factor; BDNF, brain-derived neurotrophic factor; VEGFR2, vascular endothelial growth factor receptor 2; ECA, external carotid artery

* Corresponding author.
E-mail address: chenxiangyyfey@163.com (X. Chen).

https://doi.org/10.1016/j.expneurol.2018.12.005
Received 17 September 2018; Received in revised form 2 December 2018; Accepted 10 December 2018
Available online 13 December 2018
0014-4886/ © 2018 Elsevier Inc. All rights reserved.

Ischemic penumbra (IP) was first proposed by Astrup et al. (1981)). It was defined as a region of reduced cerebral blood flow (CBF) with absent, spontaneous, or induced electrical potentials that still maintained ionic homeostasis and transmembrane electrical potentials. It is located in the peri-infarct area and Fig.2 shows schematic diagram of ischemic core and ischemic penumbra (Collaco-Moraes et al., 1994; Ashwal et al., 1998; Zhao et al., 2017). During the first few hours after stroke, it is highly likely that molecular events in the penumbra mostly comprise injury, and most would agree that a few weeks later they mainly comprise repair. Therefore, the penumbra is not just passively dying over time. It is also actively recovering (Lo, 2008). It is known that the evolution of stroke plumbing problems affects the electrical system of the brain through ischemia-induced loss of synapses and circuits (Dirnagl et al., 1999). The majority of synapses are found on dendrites and are a major determinant of how neurons integrate and process incoming information; thus, dendritic remodeling in the penumbra plays an integral role in stroke recovery (Hickmott and Ethell, 2006). Dendritic spines are the recipients of most excitatory synapses, where they participate in the transmission and integration of synaptic signaling (Harris and Kater, 1994). Postmortem histological studies have shown that stroke can induce changes in dendritic branch complexity and spine density (Corbett et al., 2006). Additionally, dendritic spine density is closely related to the expression of synaptic protein markers, such as synapsin I (SYN I) and post-synaptic density protein 95 (PSD95) (Toy et al., 2014). SYN I is expressed in neurons and known as a specific presynaptic marker (Wiedenmann and Franke, 1985). PSD-95 is a protein that is localized to the postsynaptic density of asymmetric synapses (Aoki et al., 2001). MAP-2 is selectively concentrated in the neuron body and dendrites, which can be an indication of compensatory dendrite reconstruction in the remaining neurons (Li et al., 1998; Garcia et al., 2012). Moreover, after stroke, peri-infarct dendrites are exceptionally plastic, as manifested by a dramatic increase in the rate of spine formation that is maximal at 1–2 weeks (5–8-fold increase) and still evident 6 weeks (Brown et al., 2007). When challenged with ischemic stroke, dendrites in the penumbra show a series of changes with morphologic modifications (Brown and Murphy, 2008). (See Table 1.)

It has been demonstrated that physical exercise can enhance neurogenesis and growth factor expression, synaptogenesis, neurogenesis and angiogenesis (Pang et al., 2017; Zhao et al., 2017). Treadmill exercise has a significant therapeutic effect on facilitating expression of PSD-95, SYN I and increasing number of dendritic spines in the striatum (Shin et al., 2016). Additionally, treadmill exercise has beneficial effects on working memory in the mouse barrel cortex by suppressing stress-induced dendritic spine elimination (Chen et al., 2017). Despite these effects in central nervous system diseases, very little is known about whether treadmill exercise mediates the effects on dendrites and dendritic spine development in the penumbra after focal ischemia.

Caveolin-1, a major structural protein of caveolae, is present at excitatory synapses (Petralia et al., 2003) and binds directly to the calmodulin-dependent scaffolding protein- striatin (Gaillard et al., 2001), which acts as a signaling platform in dendritic spine signal transduction (Benoist et al., 2006), and SNAP25, which forms a complex with caveolin-1 presynaptically for synaptic potentiation (Braun and Madison, 2000). Recently, both in vivo and in vitro studies have reported that neuron-targeted overexpression of caveolin-1 achieved by linking it to a neuron-specific synapsin promoter (synapsin-driven caveolin-1) enhances dendritic growth and arborization (Head et al., 2011; Mandyam et al., 2017). Vascular endothelial growth factor (VEGF) is closely related to neurite outgrowth and dendritic spine formation. As previously reported, olfactory bulb interneurons from VEGF-inhibited mice display markedly fewer developed dendritic trees and a reduced total dendritic length and number of dendritic branching points. (Licht et al., 2010). It has been demonstrated that VEGF exerts its antidepressant-like effects through the activation of FIK-1 by promoting dendritic spine formation. Thus, VEGF is an important signaling molecule during dendritic development (Huang et al., 2012). In primary neuronal cultures, VEGF causes a significant neural outgrowth and increased cell size compared with untreated neurons (Rosenstein et al., 2003). We have previously shown that the caveolin-1/VEGF signaling pathway shows improved functional recovery in response to treadmill exercise-induced angiogenesis and neurogenesis in penumbra after ischemia stroke (Gao et al., 2014; Zhao et al., 2017). In the central nervous system, angiogenesis and neurogenesis are tightly associated with synaptic and dendritic plasticity. (Carmeliet and Tessier-Lavigne, 2005).

Table 1
Modified Neurological Severity Scoring.

Motor tests	
Raising rat by tail	3
Flexion of forelimb	1
Flexion of hindlimb	1
Head moved 10° to vertical axis within 30 s	1
Placing rat on floor (normal = 0; maximum = 3)	3
Normal walk	0
Inability to walk straight	1
Circling toward paretic side	2
Falls down to paretic side	3
Sensory tests	2
Placing test (visual and tactile test)	1
Proprioceptive test (deep sensation, pushing paw against table edge to stimulate limb muscles)	1
Beam balance tests (normal = 0; maximum = 6)	6
Balances with steady posture	0
Grasps side of beam	1
Hugs beam and 1 limb falls down from beam	2
Hugs beam and 2 limbs fall down from beam, or spins on beam (> 60 s)	3
Attempts to balance on beam but falls off (> 40 s)	4
Attempts to balance on beam but falls off (> 20 s)	5
Falls off; no attempt to balance or hang on to beam (< 20 s)	6
Reflex absence and abnormal movements	4
Pinna reflex (head shake when auditory meatus is touched)	1
Corneal reflex (eye blink when cornea is lightly touched with cotton)	1
Startle reflex (motor response to a brief noise from snapping a clipboard paper)	1
Seizures, myoclonus, myodystony	1
Maximum points	18

One point is awarded for inability to perform the tasks or for lack of a tested reflex: 13–18, severe injury; 7–12, moderate injury; 1–6, mild injury.

Currently, first, it is not known whether treadmill exercise promotes dendritic plasticity in the penumbra after ischemic stroke. Second, the presence of a relationship between treadmill exercise and caveolin-1/VEGF signaling pathways on dendritic and synaptic plasticity remains unknown. Therefore, we hypothesized that the neuroprotective effects of treadmill exercise involve dendritic/synaptic plasticity and that caveolin-1/VEGF signaling plays a positive role in exercise-mediated dendritic and synaptic plasticity.

In this study, we show that treadmill exercise can promote the dendritic/synaptic plasticity. Using a specific inhibitor against caveolin-1 to elucidate the role of the caveolin-1/VEGF signaling pathway in treadmill exercise-stimulated dendritic plasticity and synaptogenesis, we further demonstrated a close correlation between the effects of treadmill exercise and caveolin-1/VEGF signaling on dendritic and synaptic plasticity.

2. Materials and methods

2.1. Reagents and antibodies

Anti-MAP2 and Anti-synapsin I were purchased from Proteintech (Rosemont, IL, USA). Anti-caveolin-1, Anti-VEGF and Anti-PSD95 were purchased from Abcam (330 Cambridge Science Park, Cambridge, UK). Tubulin antibody was purchased from Affinity Biosciences (Cincinnati, OH, USA). A FD Rapid Golgi-Stain Kit was purchased from FDNeuroTechnologies, Inc. (Guilford, MD, USA). Fetal bovine serum

(FBS) was purchased from Invitrogen (Carlsbad, CA, USA). An enhanced chemiluminescence (ECL) kit was purchased from Bio-Rad (Hercules, CA, USA), and all the other reagents were purchased from Sigma-Aldrich (St. Louis, MO, USA) unless otherwise specified.

2.2. Animals

A total of 191 adult (8-week-old) Sprague-Dawley male rats (Estrogen in female rats has an important impact on the area of cerebral infarction.) weighing 250–280 g were purchased from Shanghai Laboratory Animal Center (Shanghai, China). All the experimental protocols were approved by the Animal Research Committee of Wenzhou Medical University and followed the National Institutes of Health Guide for the Care and Use of Laboratory Animals. They were housed in a controlled environment (4 animals per cages, 55 ± 5% relative humidity, 22 °C, 12: 12-h light/dark cycle) and provided with free access to food and water. Rats were randomly divided into eleven groups: Sham-operated ($n = 19$; group S); Inhibitor treated shams ($n = 20$; 7 and 28 days, groups SI7 and SI28); Model ($n = 38$; 7 and 28 days, groups M7 and M28); Treadmill exercise trained models (n = 38; 7 and 28 days, groups EM7 and EM28); Inhibitor treated models (n = 38; 7 and 28 days, groups IM7 and IM28); Inhibitor treated and treadmill exercise trained models (n = 38; 7 and 28 days, groups IEM7 and IEM28). Studies were designed and conducted according to following criteria (Saver et al., 2009): (1) Randomization: all animals were randomly assigned to treatment groups. (2) Allocation concealment: the researcher performing the surgery or treatment application was blinded to the procedures. Researchers performing mNSS test, HE staining, infarct volume assessment, western blot; immunofluorescence; transmission electron microscopy and Golgi-Cox staining were also blinded to the procedures. (3) Blinded assessment of outcome: two independent researchers performing the image analysis and outcome assessment were blinded to all surgical procedures and treatment applications. Notably, rats were anesthetized with 3% isoflurane vaporized in 30% O2/70%N2 until they were unresponsive to the tail pinch test and then fitted with a nose cone blowing 1.5% isoflurane for anesthesia maintenance during surgery. Additionally, all rats were narcotized by an intraperitoneal injection of 10% chloral hydrate (5 ml/kg) before sacrifice.

2.3. MCAO model of focal brain ischemia

Briefly, after rats were anesthetized, we isolated the common carotid artery (CCA) and external carotid artery (ECA) from the surrounding connective tissues. We opened a small nick in the ECA stump and inserted a fine silicon-coated surgical nylon monofilament (0.36 ± 0.02 mm; L3600, Jia Ling Biotechnology Co., Ltd., Guangzhou, China) into the left internal carotid artery lumen through the ECA and gently inserted it into the internal carotid artery (ICA) up to a point approximately 18 mm distal to the bifurcation of the carotid artery to block the middle cerebral artery (MCA). The filament was fixed in place, and the animal was allowed to recover from anesthesia. After 2 h, the nylon monofilament was withdrawn to permit reperfusion. Rats in the S group were treated identically, except for inserting the surgical nylon monofilament.

2.4. Treadmill exercise and injection of the caveolin-1 inhibitor

The exercise program utilizing the ZH-PT Treadmill (Huaibei Zhenghua Bio Equipment Co., Ltd., Anhui, China) was designed based on our previous study. Before MCAO, the animals were subjected to an adaptive treadmill training over a 3-day acclimation period. At 2 days after MCAO, rats in the exercise (EM and IEM) groups were subjected to a treadmill exercise program (0° slope, 8 m/min, 30 min/day, 5 days/week) for a period of 7 or 28 days.

Rats in the SI; IM and IEM groups were injected intraperitoneally with a specific inhibitor of caveolin-1, daidzein, (0.4 mg/kg) every 24 h following reperfusion as previously described. Rats in the other groups (S, M and EM) were injected simultaneously with an equal volume of saline.

Table 2
Modified Neurological Severity Scores post MCAO.

Groups	N	1 day	7 days	28 days
S	19	0	0	0
SI	20	0	0	0
M	38	5.41 ± 0.94*	4.94 ± 0.97*	3.41 ± 0.80*Δ
EM	38	5.53 ± 0.87	4.06 ± 0.90#	2.29 ± 0.77#¥
IM	38	5.47 ± 0.94	5.65 ± 0.79#	2.65 ± 0.86#
IEM	38	5.29 ± 0.99	4.88 ± 0.93&	2.71 ± 0.85&

Data were presented as mean ± SD, ANOVA.
* $p < 0.05$ as compared to the same period of S.
# $p < 0.05$ as compared to the same period of M.
& $p < 0.05$ as compared to the same period of EM.
Δ $p < 0.05$ as compared to the M group at 7 days.
¥ $p < 0.05$ as compared to the EM group at 7 days.

2.5. Neurological function test

The modified neurological severity score (mNSS) test (Chen et al., 2001) was measured at 1d, 7 d and 28 d after MCAO by two independent examiners who were blinded to the treatment groups to score recovery in an open field. The mNSS is a composite of motor, sensory, reflex, and balance tests and is graded on a scale from 0 to 18 (normal score 0, maximal deficit score 18). The higher the score is, the more severe is the injury (Table 1).

2.6. Infarct volume assessment

Rats were sacrificed by decapitation 7 days or 28 days after MCAO to evaluate the volume of cerebral infarction. Serial sections from bregma +4.0 to −6.0 mm were selected for Nissl staining to measure the infarct volume in the ipsilateral hemisphere. Nissl staining was performed with 0.1% cresyl violet according to a previously reported procedure (Zhang et al., 2013). For quantification of infarct volume, five successive coronal sections at 2.0 mm intervals from bregma (+4.0 to −6.0 mm) were selected. The volumes of the ipsilateral and the contra-lateral hemisphere were counted as previously mentioned and relative infarct volume was described as a percentage of the contralateral hemisphere: contralateral hemispheric volume - non-infarcted tissue in the ipsilateral hemisphere)/contralateral hemispheric volume (Swanson et al., 1990).

2.7. Tissue preparation and HE staining

Four rats from each group were sacrificed at 7 and 28 days after MCAO. Briefly, under deep anesthesia with 10% chloral hydrate (5 ml/kg body weight), rats were transcardially perfused with 0.9% sodium chloride at 4 °C, followed by 4% paraformaldehyde in 0.1 M phosphate buffer (PB, pH 7.4). The brains were then removed, kept in the same fixative for 24 h at 4 °C, and immersed in 0.1 M phosphate-buffered 20% and 30% sucrose overnight at 4 °C, respectively. Coronal sections (10 μm thick) of the brains containing ischemic penumbra were cut using a cryostat.

HE staining adopts the usage of hemalum. Hemalum stains the nuclei of cells blue. Then, an aqueous eosin counterstains eosinophilic structures in various shades of red, pink and orange. We used an Olympus BH-2 microscope (Olympus Optical, London, UK) to capture the images.

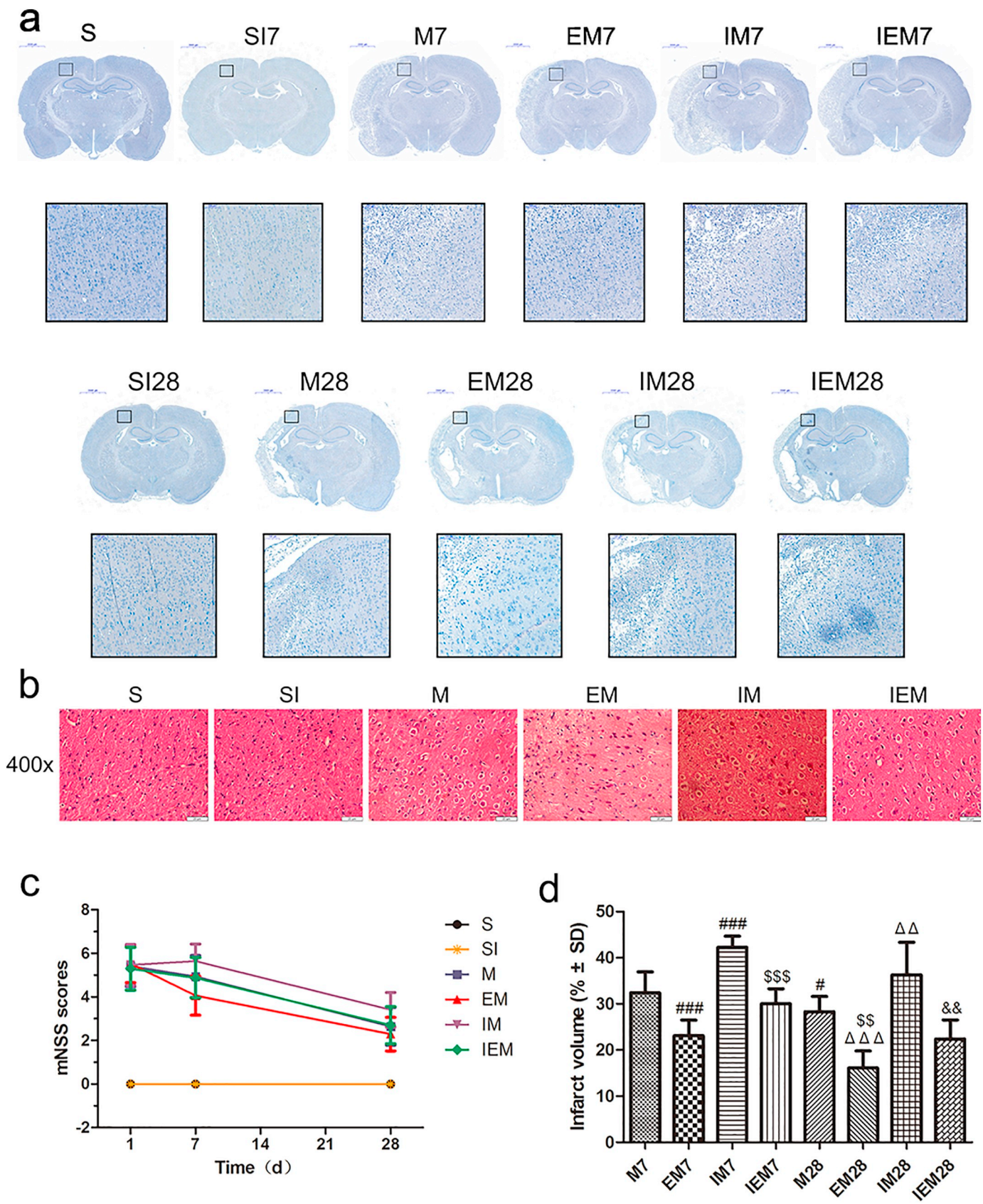

Fig. 1. Treadmill training decreased infarct volume; the damage of tissue structure and ameliorated neurologic impairment, while inhibitor increased infarct injury. a Infarct volumes. b HE staining at 7 days. Scale bars are 20 μm (400×). c Neurological scores in different groups. d Percentage of infarct volume in each group; *columns* represent mean ± SD, $n = 5$. $^{\#}p < 0.05$ versus the M7 group; $^{\$}p < 0.05$ versus the EM7 group, $^{\Delta}p < 0.05$ versus the M28 group, $^{\&}p < 0.05$ versus the EM28 group. ($^{\#}p$, $^{\$}p$, $^{\Delta}p$, $^{\&}p < 0.05$; $^{\#\#}p$, $^{\$\$}p$, $^{\Delta\Delta}p$, $^{\&\&}p < 0.01$; $^{\#\#\#}p$, $^{\$\$\$}p$, $^{\Delta\Delta\Delta}p$, $^{\&\&\&}p < 0.001$).

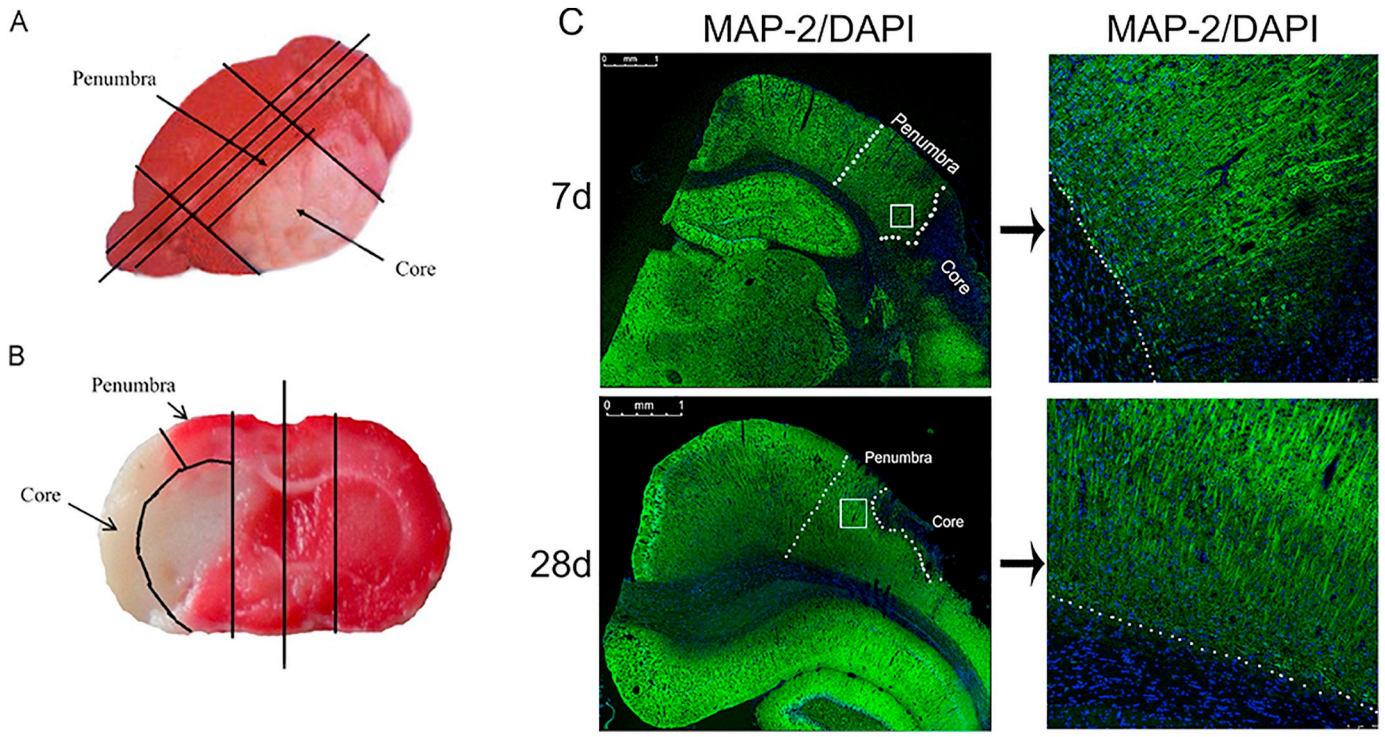

Fig. 2. Schematic diagram of ischemic core and ischemic penumbra. A, B Site of core and penumbra area (picture from the previous paper of our team); C A representative fluorescence image of MAP-2 in the penumbra at 7 days and 28 days after MCAO.

2.8. Immunofluorescence

Prepared sections were naturally air-dried and then washed in 0.1 M borate solution (pH 8.6) twice for 10 min. The sections were then washed three times in 0.01 M PBS, blocked with 10% normal goat serum at room temperature for 1 h, and incubated with rabbit Anti-PSD95 and rabbit Anti-MAP2 overnight at 4 °C. A goat anti-rabbit antibody conjugated to green fluorescent protein (GFP) Alexa Fluor 488 (1:100, Yesen, Shanghai, China) was used to show immunoreactivity. Nuclei were counterstained with 4,6-diamidino-2-phenylindole (DAPI). Negative control sections were incubated with 0.01 M PBS instead of primary antibodies and showed no positive fluorescent signals. Combining the previous exploration of our team with the classical dissection method, observation area of ischemic penumbra is as follows (Gao et al., 2014) (Fig.2c) All sections were observed with a microscope (BX51, Olympus). Positive cells in five non-overlapping fields (×400 magnifications) were enumerated using Image-Pro Plus 6.0 analysis software.

2.9. Western blot analysis

As previously reported, coronal sections were taken 4 mm and 9 mm from the front of the frontal lobe, and the middle brain tissue block was taken. We identified the midline between the two hemispheres and then made a longitudinal cut approximately 1.5–2 mm from the midline through each hemisphere. We then made a transverse diagonal cut at approximately the “10 o'clock” position to separate the core (ie, striatum and overlying cortex) from the penumbra (adjacent cortex) (Ashwal et al., 1998) (Fig.12a, b). Approximately 100 mg of brain tissue was homogenized in ice-cold RIPA buffer containing protease inhibitor cocktail (10 ul/ml) and PMSF. Equal amounts (50 μg) of proteins were separated by 10% SDS polyacrylamide gel electrophoresis and transferred to PVDF membranes. Nonspecific sites were blocked with 5% nonfat milk in TBS with 0.05% Tween 20 (TBST) for 2 h, rinsed and incubated overnight at 4 °C with primary antibodies, including caveolin-1, VEGF, PSD95, SYN I, MAP2, and Tubulin. The membranes were washed three times with TBST and treated with horseradish peroxidase-conjugated secondary antibodies (1:5000, EarthOx, LLC) for 2 h at room temperature. The blots were soaked in Super Signal chemiluminescent substrate and visualized using a UVP gel-imaging system (Upland, CA, USA). Densitometric analysis was performed using AlphaEaseFC (version 4.0).

2.10. Transmission electron microscopy

Rats were sacrificed at 7 and 28 days after MCAO, and tissue samples were collected from the ischemic penumbra. Following fixation in 2.5% (*w/v*) glutaraldehyde overnight, ischemic penumbra tissues were post-fixed in 2% (*v*/v) osmium tetroxide and blocked with 2% (v/v) uranyl acetate. Following dehydration in a series of acetone washes, the tissues were embedded in Araldite for coronal sections. Semi-thin section and toluidine blue staining were performed for observation of location. Finally, ultra-thin sections of at least three blocks per sample were cut and observed using a Hitachi TEM.

2.11. Golgi-cox staining procedure and selection criteria for pyramidal cells

At 7 d and 28 d after MCAO, rats in each group ($n = 4$) were injected intraperitoneally with a lethal dose of chloral hydrate to induce anesthesia. The brains were removed as soon as possible without perfusion and the tissue rinsed in double-distilled water for 2–3 s to remove blood from the surface. The Rapid Golgi Stain Kit (FD Neuro Technologies) was used for the tissue preparation and staining procedures. The whole Golgi-Cox staining procedure was conducted in strict accordance with the manufacturer's user manual and material safety data sheet. A series of 200 μm thick coronal sections was sliced from the caudal forelimb region of the motor cortex (approximately from the bregma to +2.0 mm from the bregma) (Budantsev et al., 1993) using a microtome (Leica CM1950 cryostat; Leica Biosystems GmbH, Wetzlar, Germany).

To be included in the analysis, neurons should be selected according to specific criteria (Gonzalez et al., 2004): (1) the dendritic trees had to

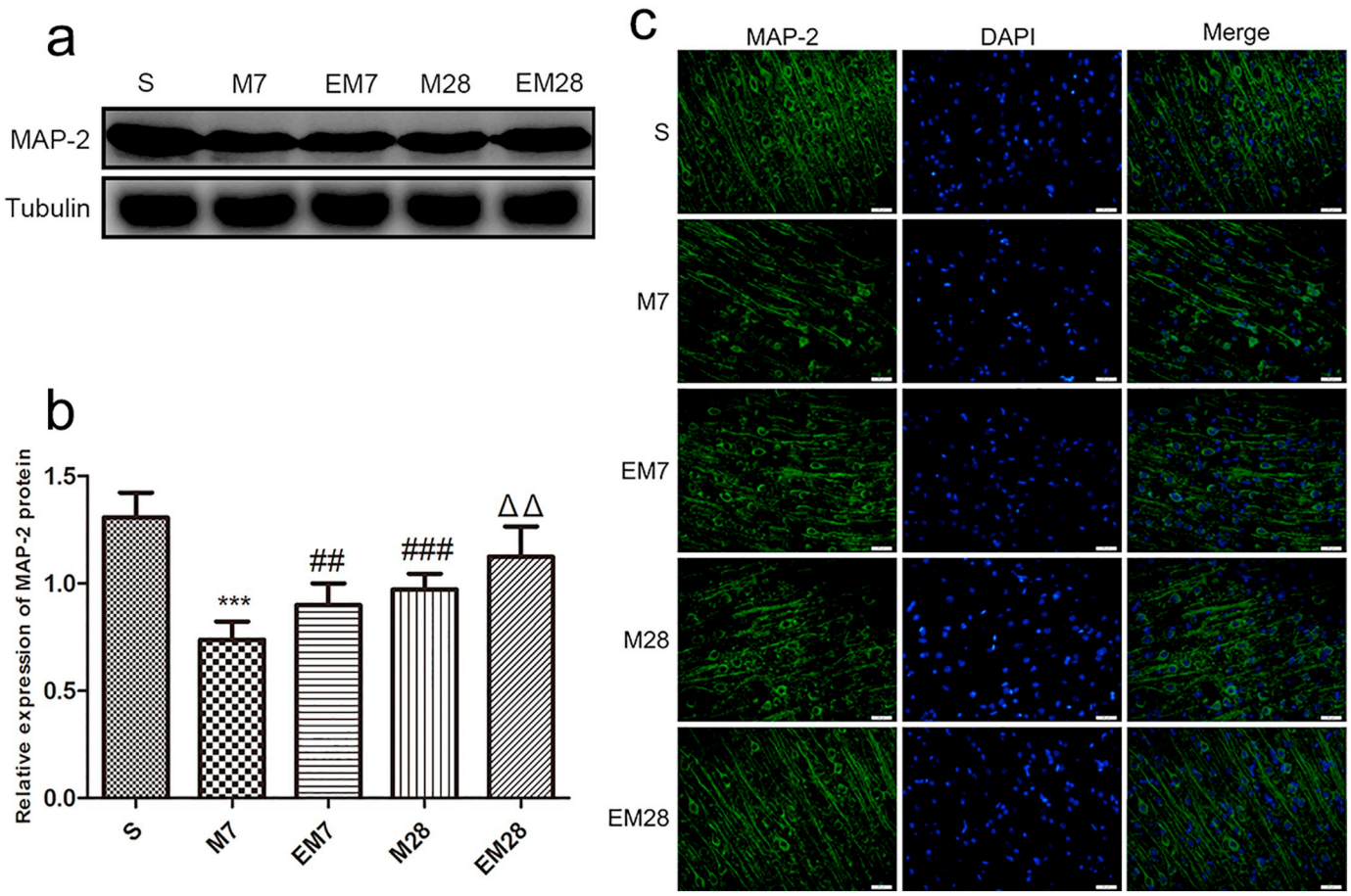

Fig. 3. Treadmill exercise up-regulated MAP-2 expression in the ischemic penumbra after MCAO. a, b Represent western blots and quantification data of MAP-2/Tubulin in each group; *columns* represent mean ± SD, $n = 5$. $^{*}p < 0.05$ versus the S group, $^{\#}p < 0.05$ versus the M7 group, $^{\Delta}p < 0.05$ versus the M28 group. c MAP-2 staining in the ischemic penumbra. Green: MAP-2; Blue: DAPI. Scale bar, 20 μm. ($^{*}p$, $^{\#}p$, $^{\Delta}p < 0.05$; $^{**}p$, $^{\#\#}p$, $^{\Delta\Delta}p < 0.01$; $^{***}p$, $^{\#\#\#}p$, $^{\Delta\Delta\Delta}p < 0.001$). (For interpretation of the references to colour in this figure legend, the reader is referred to the web version of this article.)

be well impregnated to facilitate accurate observation and analysis; (2) the cell bodies and dendrites had to be in full view and not obscured by other blood vessels, astrocytes, or clustering of dendrites from other pyramidal cells; (3) they also had to appear intact and visible in the plane of the section.

2.12. Sholl analysis

To acquire images for analysis, layer V pyramidal cells within the peri-infarct area were traced at 400× magnification. Pyramidal neurons were readily identified by their characteristic triangular soma-shape, apical dendrites extending toward the pial surface, and numerous dendritic spines. To measure the length of dendrites, Sholl analysis (Sholl, 1953) was conducted using a Sholl analysis plug-in (available at http://fiji.sc/Sholl Analysis) for ImageJ software (National Institutes of Health, Bethesda, MD, USA). The number of intersections and branches of dendrites with a series of concentric rings at 20 μm intervals from the center of the cell body was counted for each cell. The total dendritic length can also be calculated using the Sholl analysis. Five selected neurons were studied for each of the 4 animals in the different experimental groups and compared across groups using one-way ANOVA. (This method does not attempt to assess the actual total dendritic length of labeled neurons, but it has been shown to be a sensitive and reliable indicator of changes in dendritic morphology during normal development, after changes in dendritic interactions and afferent input, and after injury.)

2.13. Measurement of spine density

The dendritic spine density was analyzed for layer V pyramidal neurons within the peri-infarct area. For each cell, at least 30 μm long segments of terminal basilar densities (third order or greater) and apical densities (lower half of the apical segments) were obtained. The same cells were traced at 400× magnification. The spine number was counted, and the exact length of the dendritic segment was calculated to yield spines/10 μm data (Hurtado et al., 2007). We did not make any attempt to correct for spines that were hidden by the overlying dendrites. Therefore, the data are likely to underestimate the actual density.

2.14. Statistical analysis

Data are presented as the mean ± SD. Statistical significance was examined using one-way analysis of variance (ANOVA). p values < 0.05 were considered statistically significant. Data were analyzed using SPSS19.0 statistical software.

3. Results

3.1. Treadmill training decreased the infarct volume and damage to the tissue structure and ameliorated neurologic impairment, while the inhibitor increased infarct injury

According to the mNSS score (Table 2, Fig.1c), the functional outcome in the S and SI groups were normal (0). There were no significant

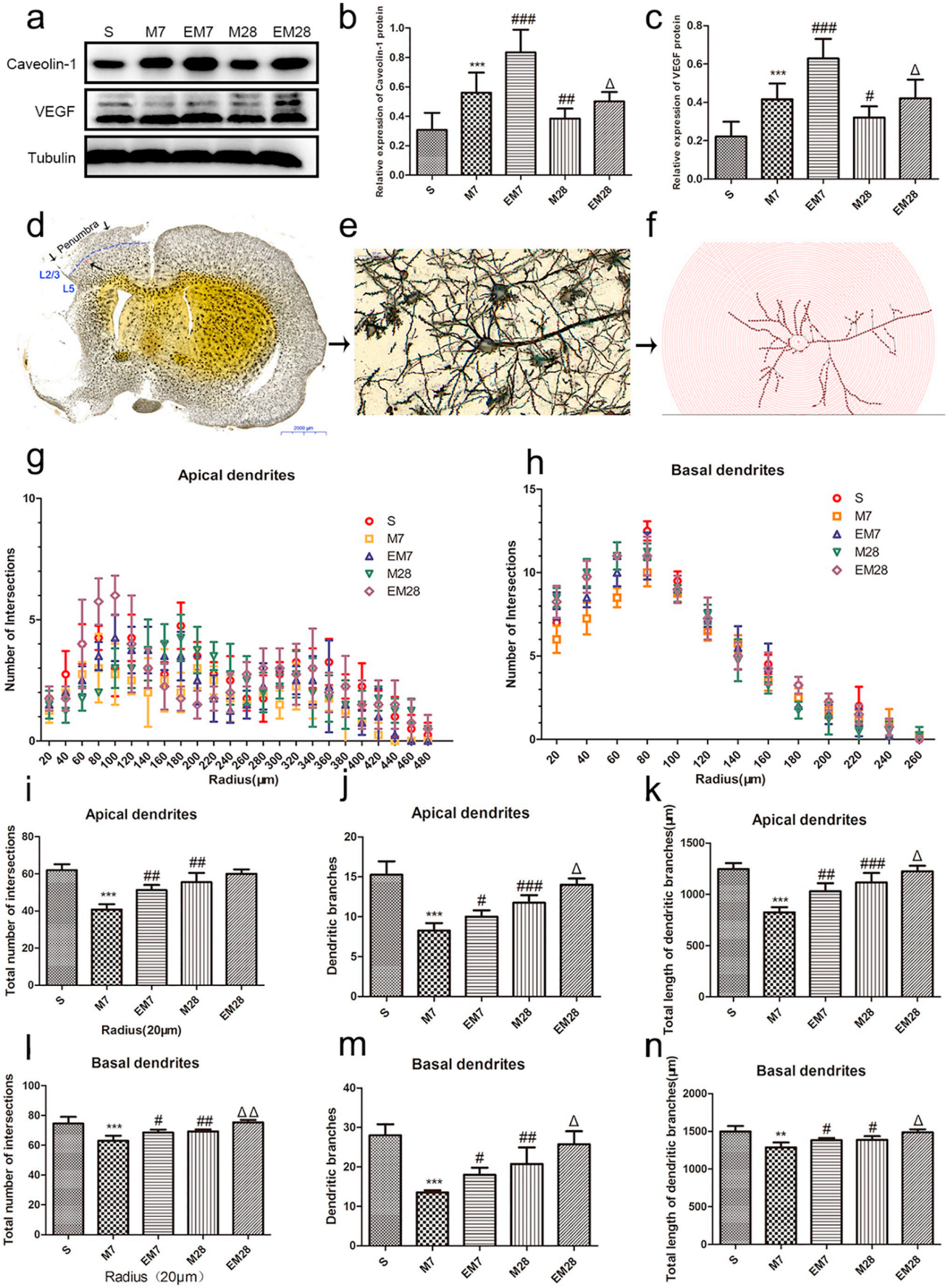

(caption on next page)

Fig. 4. Treadmill exercise promoted dendritic growth. a, b, c Represent western blots and quantification data of Caveolin1/Tubulin and VEGF/Tubulin in each group; *columns* represent mean ± SD, $n = 4$. $^{*}p < 0.05$ versus the S group; $^{\#}p < 0.05$ versus the M7 group; $^{\Delta}p < 0.05$ versus the M28 group. d, e, f Examples of reconstructed layer V pyramidal neurons and the dendritic complexity was assessed by Sholl analysis. Scale bar, 50 μm. g, h Graphs showed the distribution of dendritic intersections at increasing distance from the cell body. i, l Total number of intersection points; *columns* represent mean ± SD, n = 4. $^{*}p < 0.05$ versus the S group; $^{\#}p < 0.05$ versus the M7 group; $^{\Delta}p < 0.05$ versus the M28 group; j, m Dendritic branches. *Columns* represent mean ± SD, n = 4. $^{*}p < 0.05$ versus the S group; $^{\#}p < 0.05$ versus the M7 group; $^{\Delta}p < 0.05$ versus the M28 group; k, n The total length of dendritic branches; *columns* represent mean ± SD, n = 4. $^{*}p < 0.05$, versus the S group; $^{\#}p < 0.05$ versus the M7 group; $^{\Delta}p < 0.05$ versus the M28 group. ($^{*}p$, $^{\#}p$, $^{\Delta}p < 0.05$; $^{**}p$, $^{\#\#}p$, $^{\Delta\Delta}p < 0.01$; $^{***}p$, $^{\#\#\#}p$, $^{\Delta\Delta\Delta}p < 0.001$).

differences in the neurologic score among the four other groups at 1 day after MCAO ($p > 0.05$), and the scores of the components subsequently gradually decreased. At 7 or 28 days after MCAO, the scores for the EM group were lower than for the M group during the same period (EM7 vs. M7: $p = 0.004$; EM28 vs. M28: $p = 0.0003$), and scores for the IM group were higher than those for the M group (IM7 vs. M7: $p = 0.02$; IM28 vs. M28: $p = 0.012$). Compared with the EM group, the IEM group exhibited significantly improved neurological statuses (IEM7 vs. EM7: $p = 0.007$; IEM28 vs. EM28: $p = 0.020$). Compared with the M7 or EM7 group, the M28 group or EM28 group exhibited significantly improved neurological statuses ($p < 0.0001$).

As shown in Fig.1a, d and Table 3, compared with M group, the EM group had smaller infarct volumes during the same period ($p < 0.0001$), while the IM group had larger infarct volumes (IM7 vs. M7: $p < 0.0001$; IM28 vs. M28: $p = 0.008$). The IEM group had larger infarct volumes compared with the EM group (IEM7 vs. EM7: $p < 0.0001$; IEM28 vs. EM28: $p = 0.001$). In terms of the two M groups at different time periods, the M28 group had significantly smaller infarct volumes compared with the M7 group ($p = 0.031$), and the same trend was observed in the EM group during two different time periods ($p = 0.005$).

The neuronal morphology of the rat brain was observed after MCAO by hematoxylin and eosin (HE) staining (Fig. 1b). No infarcts were found in the brain slices from the S group, while the infarct site was observed in the ischemic area in the other groups. Brain tissues from the EM group showed a more regular arrangement than those from the M group, while tissues from the IM group showed more severe damage with multiple vacuolated interspaces and dead neurons.

3.2. Treadmill exercise promoted dendritic growth, dendritic spine formation and synaptic plasticity, as well as the upregulation of caveolin-1 and VEGF in the ischemic penumbra after MCAO

3.2.1. Treadmill exercise promoted dendritic growth

To investigate the effect of treadmill exercise on dendritic growth, the expression level of MAP-2 in the penumbra and dendritic characteristics (the total number of intersections, total length of dendritic branches and total dendritic branches of both apical and basal dendrites) from layer V pyramidal neurons in the penumbra were analyzed. Western blot and immunofluorescence analysis revealed that ischemic reperfusion severely decreased the expression of MAP-2 compared with the S group (Fig. 3a, b, c) ($p < 0.0001$). At 7 or 28 days after MCAO, compared with the M group, the expression level of MAP-2 in the EM group was significantly increased (EM7 vs. M7: $p = 0.002$; EM28 vs. M28: $p = 0.004$). Moreover, the level of MAP-2 in the M28 group was significantly higher than in the M7 group ($p < 0.0001$).

Golgi-Cox staining clearly filled the dendritic shafts and spines of neurons from layer V pyramidal neurons (Fig. 4d, e, f). Ischemic reperfusion injury affected the total number of intersections in both apical and basal dendrites compared with the S group (Fig. 4g, h, i, l) (apical: $p = 0.0001$; basal: $p < 0.0001$). Compared with the M group, the total intersections of both apical and basal dendrites in the EM group were increased during the same period (EM7 vs. M7, apical: $p = 0.002$; basal: $p = 0.015$; EM28 vs. M28, apical: $p > 0.05$; basal: $p = 0.009$). Furthermore, Sholl analysis also revealed an increase in the total intersections of apical and basal dendrites in the M28 group with respect to the M7 group (apical: $p = 0.002$; basal: $p = 0.007$).

Regarding total dendritic branches, ischemia-reperfusion injury significantly decreased both apical and basal dendritic branches of layer V neurons in the penumbra with respect to the S group (Fig. 4j, m) ($p < 0.0001$). We further observed the effect of treadmill exercise on the dendritic branches. Compared with the M group, the total branches of both apical and basal dendrites were significantly increased in the EM group during the same period (EM7 vs. M7, apical: $p = 0.04$; basal: $p = 0.04$; EM28 vs. M28, apical: $p = 0.011$; basal: $p = 0.025$). Both apical and basal dendritic branches in the M28 group were clearly increased with respect to the M7 group (apical: $p = 0.0004$; basal: $p = 0.003$).

Subsequent to the analysis of total dendritic length, there was a marked reduction in both apical and basal length after MCAO compared with the S group (Fig. 4k, n) ($p = 0.0001$). Compared with the M group, the total lengths of both apical and basal dendrites were significantly increased in the EM group during the same period (EM7 vs. M7, apical: $p = 0.001$; basal: $p = 0.02$; EM28 vs. M28, apical: $p = 0.041$; basal: $p = 0.02$). Both the apical and basal dendritic total length in the M28 group were significantly increased with respect to the M7 group (apical: $p = 0.0001$; basal: $p = 0.016$).

3.2.2. Treadmill exercise promoted dendritic spine density and synaptic plasticity

After MCAO, both the apical and basal dendritic spine density of layer V neurons in the penumbra were significantly decreased compared with the S group (Fig. 5a, b c, d) ($p < 0.0001$). Compared with the M group, the dendritic spine density of both apical and basal dendrites in the EM group were significantly increased during the same period (EM7 vs. M7, apical: $p = 0.008$; basal: $p = 0.009$; EM28 vs. M28, apical: $p = 0.031$; basal: $p = 0.04$). Furthermore, we found that both the apical and basal dendritic spine density in the M28 group were markedly increased with respect to the M7 group (apical: $p = 0.001$; basal: $p = 0.02$).

To investigate the effect of treadmill exercise on synaptic plasticity, we detected the changes in the synapse and marker synapse proteins (PSD95 and SYN I) (Fig. 5e, f, g, h). Compared with the S group, the expression levels of both PSD95 and SYN1 were significantly decreased ($p < 0.0001$). Compared with the M group, the level of SYN1 in the EM group was significantly decreased during the same period (EM7 vs. M7: $p\,p = 0.047$; EM28 vs. M28: $p = 0.035$). Moreover, the level of SYN1 in the M28 group was significantly augmented compared with the M7 group ($p < 0.0001$). However, treadmill exercise had a limited effect on the expression of PSD95 at 7 days after MCAO with respect to the M7 group ($p > 0.05$). Compared with the M28 group, the level of PSD95 in the EM28 group was significantly increased, while it was markedly decreased in the M7 group (EM28 vs. M28: $p = 0.008$; M7 vs. M28: $p = 0.001$). The changing trend of the synaptic structure was consistent with the neurological outcome (Fig. 5i). Compared with the S group, the M group exhibited abnormal neurons with fewer and irregular synaptic vesicles and wider synaptic clefts, while the EM group showed better statuses with an even thickness of the synaptic membrane, more synaptic vesicles and tight synaptic connections.

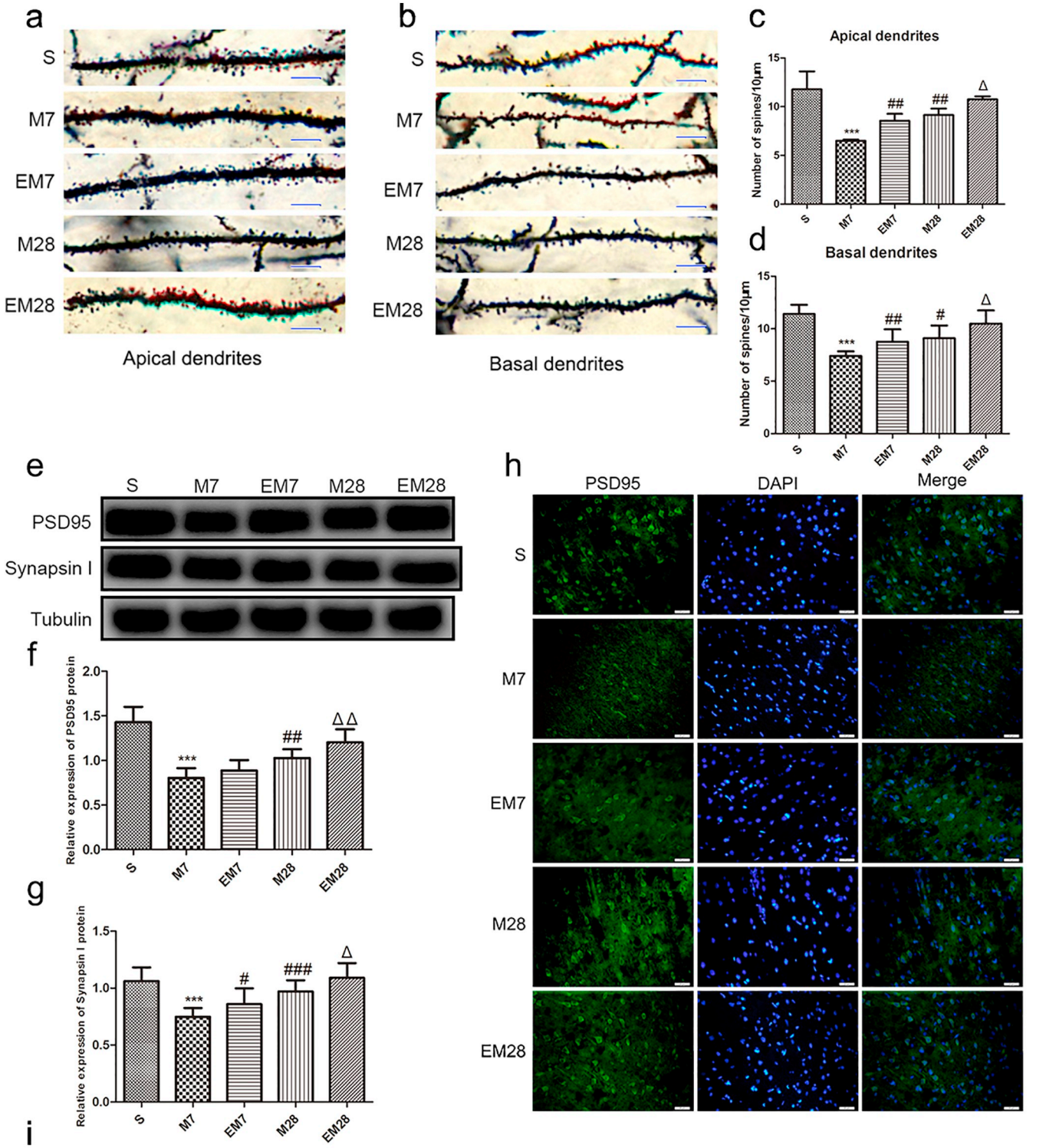

(caption on next page)

Fig. 5. Treadmill exercise promoted dendritic spine density and synaptic plasticity. a, b Examples of dendritic spines. Scale bar, 10 μm. c, d Density of dendritic spines. *Columns* represent mean ± SD, n = 4. $^{*}p < 0.05$ versus the S group; $^{\#}p < 0.05$ versus the M7 group; $^{\Delta}p < 0.05$ versus the M28 group. e, f, g Represent western blots and quantification data of PSD95 and SYN1 in each group; *columns* represent mean ± SD, n = 4. $^{*}p < 0.05$ versus the S group; $^{\#}p < 0.05$ versus the M7 group; $^{\Delta}p < 0.05$ versus the M28 group. h PSD95 staining in the ischemic penumbra. Green: PSD95; Blue: DAPI. Scale bar, 20 μm. i Transmission electron microscopy showed the synaptic structures, and the scale bars indicated 0.2 μm. ($^{*}p$, $^{\#}p$, $^{\Delta}p < 0.05$; $^{**}p$, $^{\#\#}p$, $^{\Delta\Delta}p < 0.01$; $^{***}p$, $^{\#\#\#}p$, $^{\Delta\Delta\Delta}p < 0.001$). (For interpretation of the references to colour in this figure legend, the reader is referred to the web version of this article.)

3.2.3. Molecular changes in the penumbra after MCAO following treadmill exercise

Concomitantly, we detected the expression change in caveolin-1 and VEGF (Fig. 4a, b, c). Western blot analysis revealed that the levels of both caveolin-1 and VEGF were significantly increased in the EM group at 7 or 28 days after MCAO with respect to M group rats (caveolin-1, EM7 vs. M7: $p < 0.0001$; EM28 vs. M28: $p = 0.036$; VEGF, EM7 vs. M7: $p < 0.0001$; EM28 vs. M28: $p = 0.017$), consistent with the changes in the dendritic characteristics and spine density. However, compared with the M7 group, the M28 group had significantly lower levels of both caveolin-1 and VEGF (caveolin-1: $p = 0.002$; VEGF: $p = 0.024$), in contrast to the changes in dendritic characteristics and spine density.

3.3. Inhibitor had no significant effects on synaptic and dendritic plasticity of rats in the S group

3.3.1. Inhibitor had no effects on mNSS score, infarct size and neuronal morphology of rats in the S group

The mNSS scores in the three groups were all 0 (normal) (Table 2), and none of them had infarcts (Table 3). According to the Nissl staining, there were no observable pathological changes among the three groups (Fig.1a, b).

3.3.2. Inhibitor had no significant effects on synaptic and dendritic plasticity of rats in the S group

We detected whether inhibitor can down-regulate the caveolin-1 and VEGF expression level of rats in the S group. Compared with S group, the expression level of caveolin-1 and VEGF in the SI groups slightly decreased, however, there were no statistical difference among the three groups (S vs. SI7; SI7 vs. SI28: $p > 0.05$) (Fig.6a, c, d).

We further tested the effects of inhibitor on synaptic and dendritic plasticity of the shams. Compared with S group, the expression level of MAP2, PSD95 and SYN 1 in the SI groups slightly decreased, however, there were no statistical difference among the three groups (S vs. SI7; SI7 vs. SI28: $p > 0.05$) (Fig.6b, e, f, g). Additionally, consistent with the changes in caveolin-1 and VEGF, dendritic characteristics (total length, total branches and total intersections) and spine density in the SI7 groups have no statistical reduction compared with the s groups (S vs. SI7: $p > 0.05$) (Fig.6h, i, j, k, l, m). These results excluded the possibility that the inhibitor itself may cause neurological deficits.

3.4. Inhibition of the caveolin-1/VEGF pathway abolished dendritic growth, dendritic spine formation and synaptic plasticity in the ischemic penumbra after MCAO

To determine whether the caveolin-1/VEGF pathway was related to dendritic and synaptic change, an inhibitor was utilized. As we expected, the levels of both caveolin-1 and VEGF were significantly downregulated in the IM group at 7 or 28 days after MCAO with respect to M group rats (caveolin-1, IM7 vs. M7: $p < 0.0001$; IM28 vs. M28: $p = 0.002$; VEGF, IM7 vs. M7: $p = 0.001$; EM28 vs. M28: $p = 0.004$) (Fig. 8a, b, c). Consistent with the changes in caveolin-1 and VEGF, the expression level of MAP-2 in the IM group was significantly decreased in the M group during the same period (IM7 vs. M7: $p = 0.003$; IM28 vs. M28: $p = 0.001$) (Fig. 7a, b, c).

3.5. Inhibition of the caveolin-1/VEGF pathway led to dendritic degeneration

Sholl analysis showed that total intersections of apical and basal dendrites in the IM group were significantly reduced compared with the M group during the same period (IM7 vs. M7, apical: $p = 0.017$; basal: $p = 0.003$; IM28 vs. M28, apical: $p = 0.009$; basal: $p = 0.013$) (Fig. 8d, e, f, g). The same trend was observed in the change in total length (IM7 vs. M7, apical: $p = 0.035$; basal: $p = 0.002$; IM28 vs. M28, apical: $p = 0.0001$; basal: $p = 0.033$) (Fig. 8j, k) and total branches (IM7 vs. M7, apical: $p = 0.004$; basal: $p = 0.043$; IM28 vs. M28, apical: $p = 0.017$; basal: $p = 0.027$) in comparisons of the IM and M groups (Fig. 8h, i).

3.6. Inhibiting of the caveolin-1/VEGF pathway abolished dendritic spine and synaptic construction

We further detected the expression changes in both PSD95 and SYN1, as well as the dendritic spine density at 7 or 28 days after injecting inhibitor. Compared with the M group, the expression of both PSD95 and SYN1 were clearly decreased in the IM group during the same period (PSD95, IM7 vs. M7: $p = 0.008$; IM28 vs. M28: $p = 0.018$; SYN1, IM7 vs. M7: $p = 0.013$; IM28 vs. M28: $p = 0.033$) (Fig. 9e, f, g, h). Similarly, rats in the IM group had fewer dendritic spines on both apical and basal dendrites with respect to the M group during the same period (IM7 vs. M7, apical: $p = 0.024$; basal: $p = 0.035$; IM28 vs. M28, apical: $p = 0.012$; basal: $p = 0.009$) (Fig. 9a, b, c, d). Concerning synaptic structure, transmission electron microscope analysis revealed that rats in the IM group showed more serious uneven thickness of the synaptic membrane, degradation of synaptic vesicles and even disappearance of synaptic connections compared with the M group (Fig. 9i).

3.7. Inhibition of the caveolin-1/VEGF signaling pathway suppressed exercise-promoted dendritic growth, dendritic spine formation and synaptic plasticity in the ischemic penumbra after MCAO

To ascertain whether the caveolin-1/VEGF signaling pathway participated in exercise-induced dendritic and synaptic plasticity, inhibitor and treadmill exercise were performed after MCAO, and Western blot analysis was employed to investigate the level of caveolin-1 and VEGF. The results showed that the inhibitor significantly suppressed the expression of both caveolin-1 and VEGF upregulated by treadmill exercise when comparing EM7 with IEM7 (caveolin-1: $p < 0.0001$; VEGF: $p = 0.001$). However, the expression of caveolin-1 was significantly increased ($p = 0.008$), while there was no significant effect on VEGF, in comparisons of EM28 and IEM28 ($p > 0.05$). Furthermore, compared with the EM7 group, the EM28 group had significantly lower levels of both caveolin-1 and VEGF (caveolin-1: $p < 0.0001$; VEGF: $p = 0.002$) (Fig. 11a, b, c).

3.8. Inhibition of the caveolin-1/VEGF pathway abolished exercise-promoted dendritic growth

To reconfirm the role of the caveolin-1/VEGF signaling pathway in exercise-improved dendritic growth, we established four groups (EM7; IEM7; EM28 and IEM28) and examined their dendritic characteristics by Western blotting, immunofluorescence and Golgi-Cox staining. The

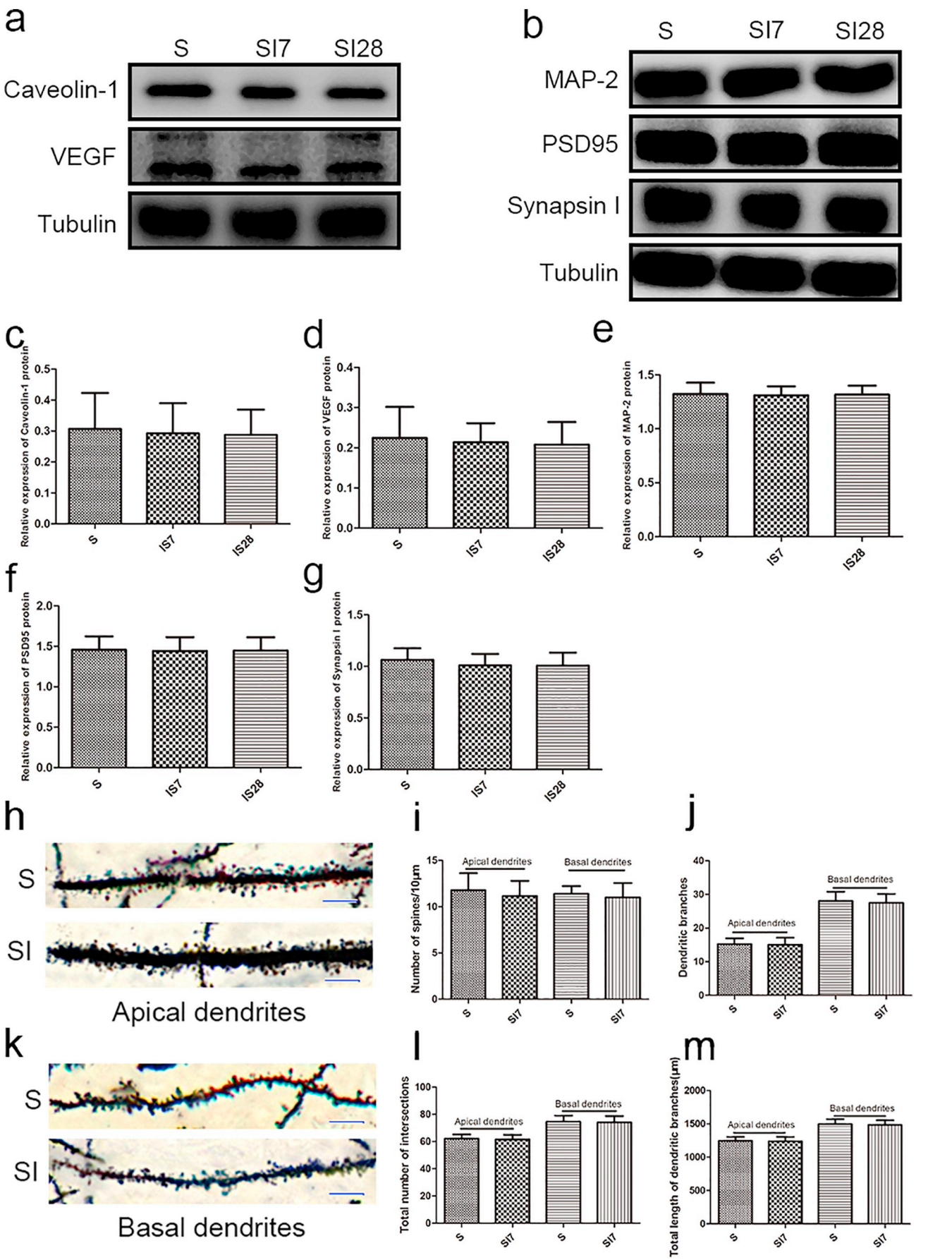

(caption on next page)

Fig. 6. Inhibitor had no significant effects on synaptic and dendritic plasticity of rats in the group S. a, b, c, d, e, f, g Represent western blots and quantification data of Caveolin1/Tubulin, VEGF/Tubulin, MAP-2/Tubulin, PSD95/Tubulin and SYN I/Tubulin in each group; *columns* represent mean ± SD, n = 4. h, k Examples of dendritic spines. Scale bar, 10 μm. i Density of dendritic spines. *Columns* represent mean ± SD, n = 4. j Dendritic branches. *Columns* represent mean ± SD, n = 4. l Total number of intersection points; *columns* represent mean ± SD, n = 4. m Dendritic branches. *Columns* represent mean ± SD, n = 4.

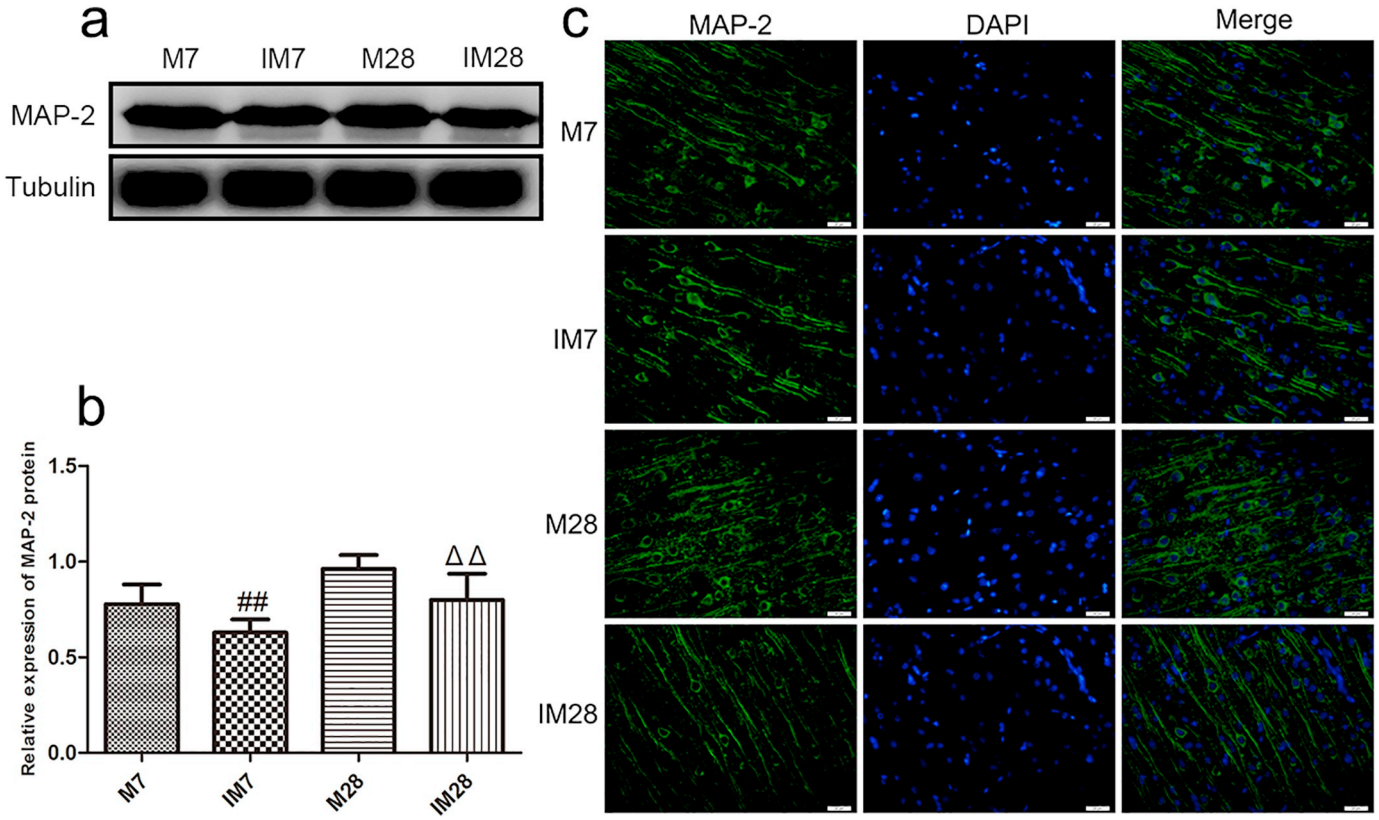

Fig. 7. Inhibitor down-regulated MAP-2 expression in the ischemic penumbra after MCAO. a, b Represent western blots and quantification data of MAP-2/Tubulin in each group; *columns* represent mean ± SD, n = 4. $^{\#}p < 0.05$ versus the M7 group, $^{\Delta}p < 0.05$ versus the M28 group. c MAP-2 staining in the ischemic penumbra. Green: MAP-2; Blue: DAPI. Scale bar, 20 μm. ($^{\#}p$, $^{\Delta}p < 0.05$; $^{\#\#}p$, $^{\Delta\Delta}p < 0.01$; $^{\#\#\#}p$, $^{\Delta\Delta\Delta}p < 0.001$). (For interpretation of the references to colour in this figure legend, the reader is referred to the web version of this article.)

immunofluorescence and Western blot assays were applied to observe MAP2-positive cell and expression levels. A lower level of MAP2 was observed in the IEM group compared with the EM group during the same period (EM7 vs. IEM7: $p = 0.045$; EM28 vs. IEM28: $p = 0.024$) (Fig. 10a, b, c).

Compared with the EM7 group, both apical and basal dendritic intersections were significantly decreased in the IEM7 group (apical: $p = 0.004$; basal: $p = 0.016$). At 28 days, there were no significant differences in apical dendritic intersections in EM28 compared with IEM28 ($p > 0.05$), while a significant decrease in basal dendritic intersections was observed by comparing EM28 with IEM28 ($p = 0.04$) (Fig. 11d, e, f, g). Moreover, both apical and basal dendritic branches were markedly decreased in the IEM group with respect to the EM group during the same period (EM7 vs. IEM7, apical: $p = 0.016$; basal: $p = 0.007$; EM28 vs. IEM28, apical: $p = 0.003$; basal: $p = 0.033$) (Fig. 11h, i). Additionally, compared with the EM group, both the apical and basal dendritic total length in the IEM group were markedly decreased during the same period (EM7 vs. IEM7, apical: $p = 0.003$; basal: $p = 0.002$; EM28 vs. IEM28, apical: $p = 0.02$; basal: $p = 0.02$) (Fig. 11j, k). Notably, compared with the EM7 group, total intersections, total length and total branches of both apical and basal dendrites were significantly improved in the EM28 group, in contrast to the trend observed for caveolin-1 and VEGF (Fig. 11e–k).

3.9. Inhibition of the caveolin-1/VEGF pathway abolished exercise-promoted dendritic spine and synaptic construction

To confirm the effect of the caveolin-1/VEGF pathway on dendritic spines and synapses, we further detected the dendritic spine density and expression changes in PSD95 and SYN I at 7 or 28 days after inhibitor injection and treadmill exercise. Compared with the EM group, the expression levels of both PSD95 and SYN1 in the IEM group were decreased during the same period (PSD95, EM7 vs. IEM7: $p = 0.025$; EM28 vs. IEM28: $p = 0.003$; SYN1, EM7 vs. IEM7: $p = 0.013$; EM28 vs. IEM28: $p > 0.05$) (Fig. 12e, f, g, h). Similarly, rats in the IEM7 group had fewer dendritic spines on both apical and basal dendrites with respect to the EM7 group (apical: $p = 0.007$; basal: $p = 0.033$). However, compared with the EM28 group, no significant reduction was observed for either the apical or basal dendritic spine density in the IEM group ($p > 0.05$) (Fig. 12a, b, c, d). Additionally, the statuses of the synapses were compared with the EM group (Fig. 12i). Similarly, and consistent with the trend of the dendritic characteristics, the changes in spine density and synaptic plasticity in the EM28 group were significantly increased with respect to the EM7 group.

4. Discussion

In this study, we found that treadmill training played a novel role in

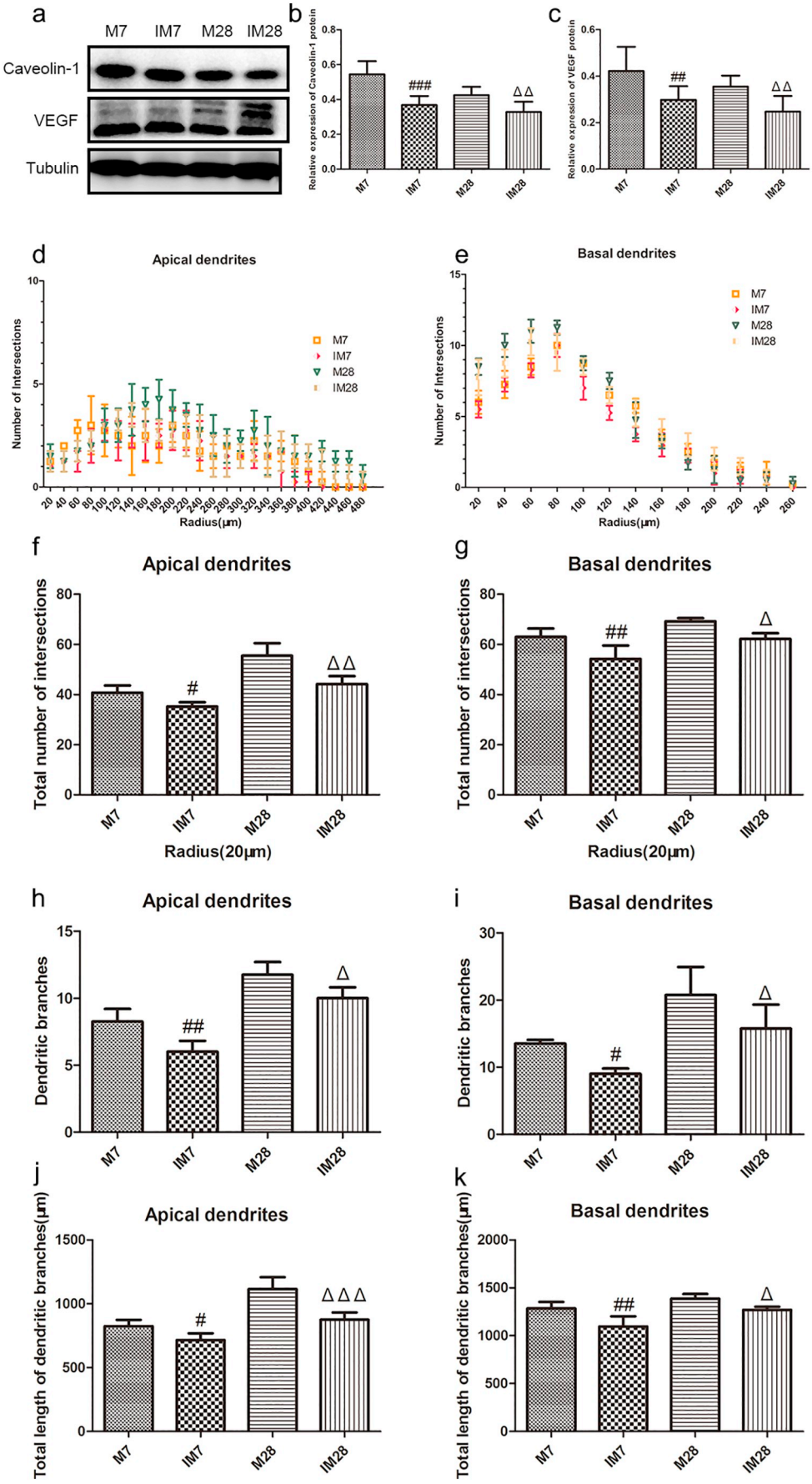

Fig. 8. Inhibition of the caveolin-1/VEGF pathway led to dendritic degeneration. a, b, c Represent western blots and quantification data of Caveolin1/Tubulin and VEGF/Tubulin in each group; *columns* represent mean ± SD, n = 4. $^{\#}p < 0.05$ versus the M7 group; $^{\Delta}p < 0.05$ versus the M28 group. d, e Graphs showed the distribution of dendritic intersections at increasing distance from the cell body. f, g Total number of intersection points; *columns* represent mean ± SD, n = 4. $^{\#}p < 0.05$ versus the M7 group; $^{\Delta}p < 0.05$ versus the M28 group; h, i Dendritic branches. *Columns* represent mean ± SD, n = 4. $^{\#}p < 0.05$ versus the M7 group; $^{\Delta}p < 0.05$ versus the M28 group; j, k The total length of dendritic branches; *columns* represent mean ± SD, n = 4. $^{\#}p < 0.05$ versus the M7 group; $^{\Delta}p < 0.05$ versus the M28 group. ($^{\#}p$, $^{\Delta}p < 0.05$; $^{\#\#}p$, $^{\Delta\Delta}p < 0.01$; $^{\#\#\#}p$, $^{\Delta\Delta\Delta}p < 0.001$).

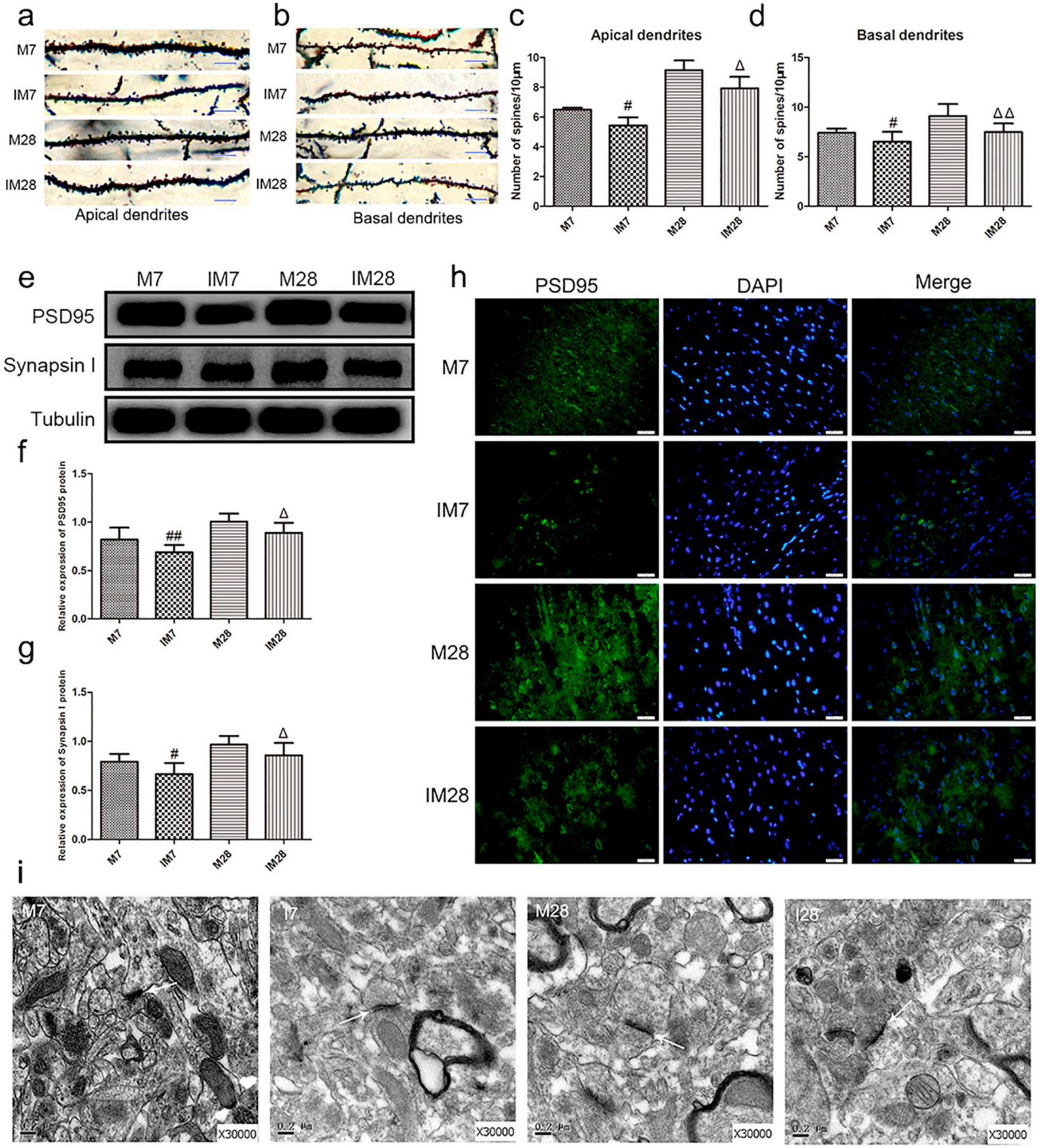

Fig. 9. Inhibition of the caveolin-1/VEGF pathway damaged dendritic spine density and synaptic plasticity. a, b Examples of dendritic spines. Scale bar,10 μm. c, d Density of dendritic spines. *Columns* represent mean ± SD, n = 4. $^{\#}p < 0.05$ versus the M7 group; $^{\Delta}p < 0.05$ versus the M28 group. e, f, g Represent western blots and quantification data of PSD95/Tubulin and SYN1/Tubulin in each group; *columns* represent mean ± SD, n = 4, $^{\#}p < 0.05$ versus the M7 group; $^{\Delta}p < 0.05$ versus the M28 group. h PSD95 staining in the ischemic penumbra. Green: PSD95; Blue: DAPI. Scale bar, 20 μm. i Transmission electron microscopy showed the synaptic structures, and the scale bars indicated 0.2 μm. ($^{\#}p$, $^{\Delta}p < 0.05$; $^{\#\#}p$, $^{\Delta\Delta}p < 0.01$; $^{\#\#\#}p$, $^{\Delta\Delta\Delta}p < 0.001$). (For interpretation of the references to colour in this figure legend, the reader is referred to the web version of this article.)

recovery from ischemic stroke - promoting dendrite outgrowth, dendritic spine formation and synapse development of layer V pyramidal neurons in the penumbra after ischemic reperfusion. Furthermore, the caveolin-1/VEGF signaling pathway could not only mediate dendritic and synaptic plasticity, but it is also a potential molecular mechanism for treadmill training to promote these effects.

The dendritic length reflected the total space for synapses, and the spine density represented the density of excitatory synapses to some

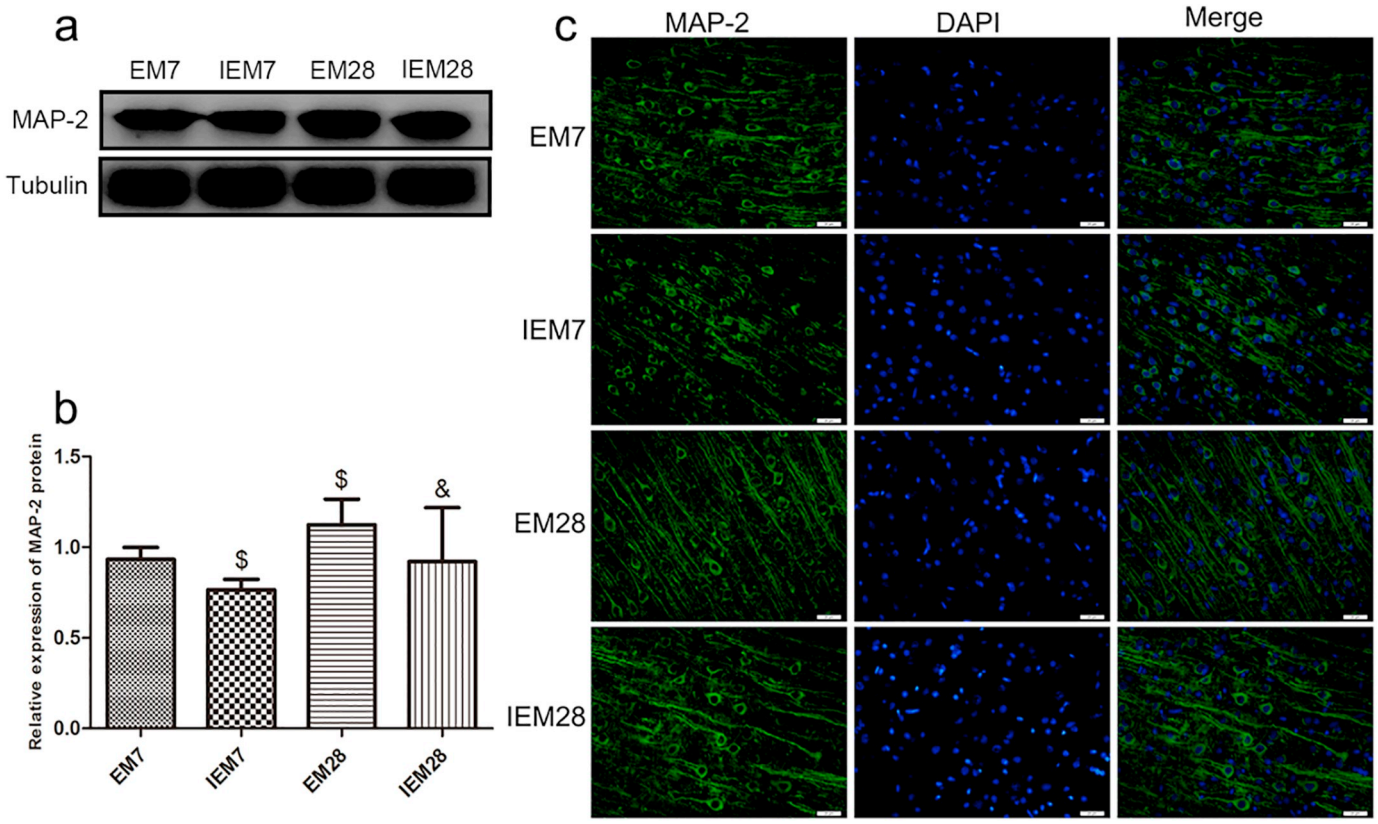

Fig. 10. Inhibition of the caveolin-1/VEGF pathway abolished exercise-promoted MAP-2 expression in the ischemic penumbra after MCAO. a, b Represent western blots and quantification data of MAP2/Tubulin in each group; *columns* represent mean ± SD, n = 4. $^{\$}p < 0.05$ versus the EM7 group, $^{\&}p < 0.05$ versus the EM28 group. c MAP-2 staining in the ischemic penumbra. Green: MAP-2; Blue: DAPI. Scale bar, 20 μm. ($^{\$}p$, $^{\&}p < 0.05$; $^{\$\$}p$, $^{\&\&}p < 0.01$; $^{\$\$\$}p$, $^{\&\&\&}p < 0.001$). (For interpretation of the references to colour in this figure legend, the reader is referred to the web version of this article.)

extent (Kolb et al., 2001). Synapses are the structural basis for the transmission, processing, and storage of information between adjacent neurons. In the acute MCAO model, dendrites and their spines represent the most vulnerable structures after the loss of blood supply. As a result, those changes disrupt the neuronal circuit and impair the function of the brain. Ischemic stroke not only causes neuronal death in the ischemic core area but also damages the structure and function of surviving neurons around the ischemic region. Although the dysfunction occurred at 7 and 28 days after cerebral ischemia-reperfusion in rats, it might recover partially over time, which may be related to the reorganization and synaptic reconnection of surviving neurons in the penumbra. In the present study, results from Golgi-Cox staining revealed that the apical and basal dendritic characteristics (dendritic intersections, dendritic length, dendritic branches and dendritic spine density) of layer V pyramidal neurons were significantly decreased in the penumbra at two time-points after MCAO, indicating the degeneration of dendrites and spines and in accordance with previous studies (Gonzalez and Kolb, 2003; Mostany and Portera-Cailliau, 2011; Jiang et al., 2012; Li et al., 2015). Comparisons of the M7 and M28 groups suggested that dendrites and dendritic spines showed a dynamic process (decreasing in the early stage and gradually increasing) after MCAO, and neurological improvement was closely related to changes in dendrites and dendritic spines. Further detection of SYN1 and PSD95 revealed that the expression level continued to grow but did not reach normal levels, consistent with the pathological damage of the ischemic penumbra and decrease in the cerebral infarction volume. This series of results indicated that dendritic plasticity and synaptic development in the penumbra played an important role in stroke recovery.

Previous studies have shown that when the brain is in a severe ischemic state, such as a 90% reduction in blood flow, irreversible dendritic damage and spine loss will occur within 10–20 min (Brown and Murphy, 2008). After cerebral ischemia, the plasticity of dendrites and dendritic spines serves as the basis for motor function recovery. For example, environmental stimulation enhances dendritic branching and length. Multiple studies have shown that sensory experience, such as exercise training, can significantly affect the dynamic changes in dendrites and dendritic spines. In the primary motor cortex of mice, exercise training can promote the formation of dendritic spines and improve the survival rate of new dendritic spines (Xu et al., 2009; Fu et al., 2012). Dendritic morphological changes were observed after physical exercise in other nervous system diseases. For instance, low-intensity exercise can increase the dendritic complexity and level of PSD95 in the hippocampus after MCAO (Shih et al., 2013). Treadmill exercise facilitates the expression of PSD95 and synaptophysin and increases the number of dendritic spines on dopaminergic neurons and fibers in mouse models of Parkinson's disease (Shin et al., 2016). In our study, treadmill exercise increased both the apical and basilar dendritic complexity and dendritic spine density in penumbra at 7 and 28 days after MCAO. Such changes in the dendritic structure would allow them to change their connectivity patterns and participate in larger and/or different neural networks in the cortex (Hickmott and Ethell, 2006). Dendritic stability was manifested by a significant increase in dendritic spine formation that peaked at 1–2 weeks, persisted for up to 6 weeks, and was specific to the peri-infarct cortex (Brown et al., 2007). Consistent with a previous study, we found that dendritic plasticity gradually increased in comparisons of the EM7 and EM28 groups. These results indicated that treadmill training could improve neurological function by promoting dendritic spine formation, dendritic extension and branching, and the effect of long-term exercise training to improve the symptoms of motor deficit after stroke was more obvious. Regarding the expression level of synaptic marker proteins, we found that PSD95 expression was elevated in EM7 compared with the M7 group,

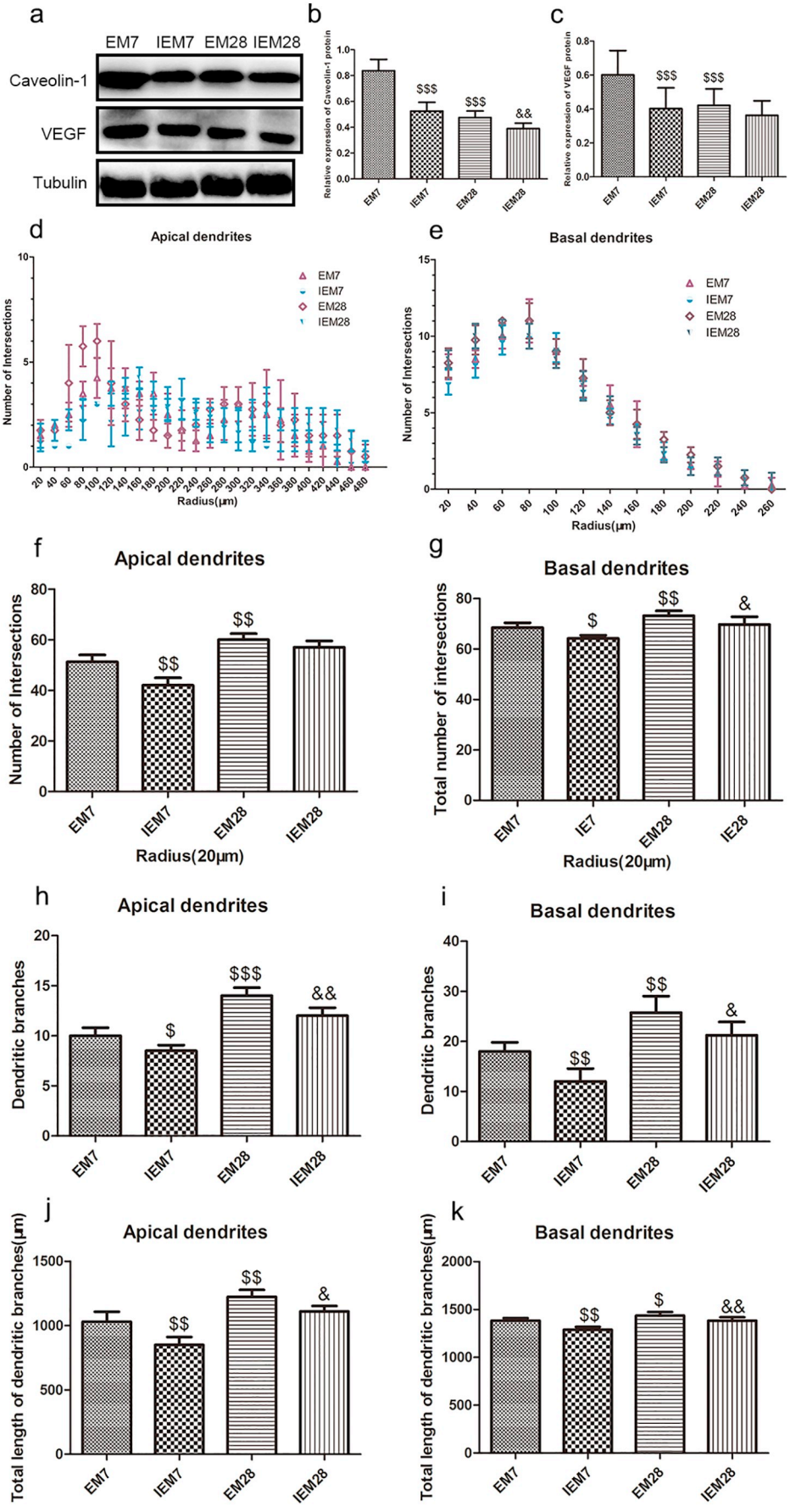

Fig. 11. Inhibition of the caveolin-1/VEGF pathway abolished exercise-promoted dendritic growth. a, b, c Represent western blots and quantification data of Caveolin1/Tubulin and VEGF/Tubulin in each group; *columns* represent mean ± SD, n = 4. $^{\$}p < 0.05$ versus the EM7 group; $^{\&}p < 0.05$ versus the EM28 group. d, e Graphs showed the distribution of dendritic intersections at increasing distance from the cell body. f, g Total number of intersection points; *columns* represent mean ± SD, n = 4. $^{\$}p < 0.05$ versus the EM7 group; $^{\&}p < 0.05$ versus the EM28 group; h, i Dendritic branches. *Columns* represent mean ± SD, n = 4. $^{\$}p < 0.05$, versus the EM7 group; $^{\&}p < 0.05$ versus the EM28 group; j, k The total length of dendritic branches; *columns* represent mean ± SD, n = 4. $^{\$}p < 0.05$ versus the EM7 group; $^{\&}p < 0.05$ versus the EM28 group. ($^{\$}p$, $^{\&}p < 0.05$; $^{\$\$}p$, $^{\&\&}p < 0.01$; $^{\$\$\$}p$, $^{\&\&\&}p < 0.001$).

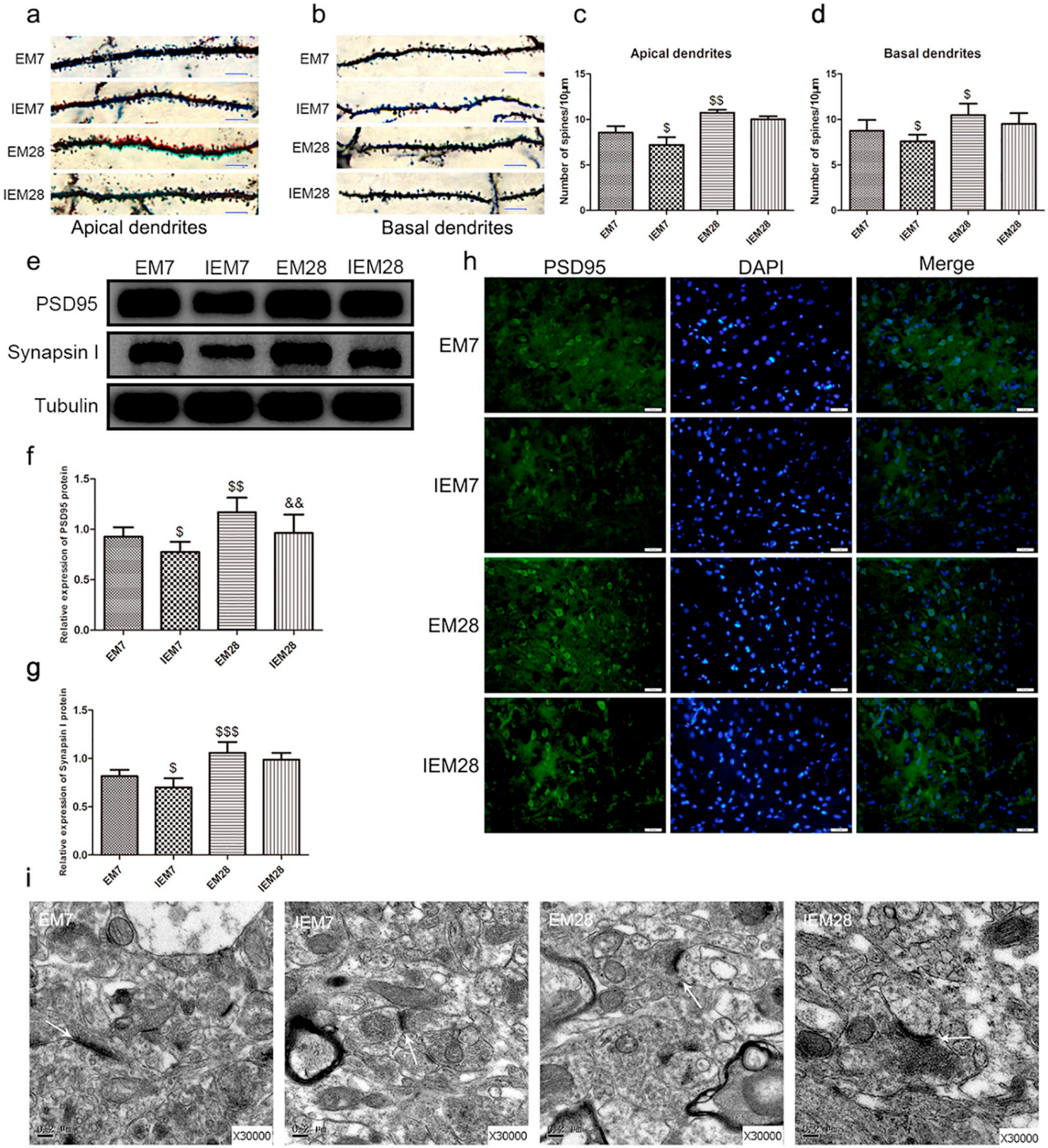

Fig. 12. Inhibition of the caveolin-1/VEGF pathway abolished exercise-promoted dendritic spine and synaptic construction a, b Examples of dendritic spines. Scale bar,10 μm. c, d Density of dendritic spines. *Columns* represent mean ± SD, n = 4. $^{\$}p < 0.05$ versus the EM7 group; $^{\&}p < 0.05$ versus the EM28 group. e, f, g Represent western blots and quantification data of PSD95 and SYN1 in each group; *columns* represent mean ± SD, n = 4. $^{\$}p < 0.05$ versus the EM7 group; $^{\&}p < 0.05$ versus the EM28 group. h PSD95 staining in the ischemic penumbra. Green: PSD95; Blue: DAPI. Scale bar, 20 μm. i Transmission electron microscopy showed the synaptic structures, and the scale bars indicated 0.2 μm. ($^{\$}p$, $^{\&}p < 0.05$; $^{\$\$}p$, $^{\&\&}p < 0.01$; $^{\$\$\$}p$, $^{\&\&\&}p < 0.001$). (For interpretation of the references to colour in this figure legend, the reader is referred to the web version of this article.)

but this difference was not statistically significant. It can be explained that, spine addition is not always coupled to synapse formation and synaptic contacts appear after the emergence of the dendritic spine (Ziv and Smith, 1996; Knott et al., 2006; Nagerl et al., 2007). Alternatively, in the Filopodia model, spines grow toward axons to make de novo synapses (Ziv and Smith, 1996), providing a good explanation for why the dendritic spines clearly increased in the EM7 group without an obvious increase in the synaptic protein. To our knowledge, the present

Table 3
Infarct Volumes.

Groups	N	7 days	28 days
S	5	0	0
SI	10	0	0
M	10	32.38 ± 4.55*	28.30 ± 3.29Δ*
EM	10	23.11 ± 3.37#	16.11 ± 3.72#¥
IM	10	42.29 ± 2.41#	36.28 ± 7.05#
IEM	10	30.03 ± 3.25&	22.38 ± 4.14&

Data were presented as mean ± SD, ANOVA.
* $p < 0.05$ as compared to the same period of S.
# $p < 0.05$ as compared to the same period of M.
& $p < 0.05$ as compared to the same period of EM.
Δ $p < 0.05$ as compared to the M group at 7 days.
¥ $p < 0.05$ as compared to the EM group at 7 days.

study is the first to investigate the effect of treadmill exercise on dendritic morphology in the penumbra after brain ischemia. Our present results revealed that treadmill exercise could enhance the dendritic complexity and dendritic spine growth in the penumbra, indicating that exercise-induced dendritic plasticity is a potential mechanism for recovery after cerebral ischemia.

Dendritic plasticity and synaptogenesis are complex processes after cerebral stroke, and their molecular mechanisms have not yet been clearly studied. Our previous in vitro and in vivo studies have shown that the caveolin-1/VEGF signaling pathway mediated neurovascular regeneration and promoted autophagy to reduce apoptosis after ischemia-reperfusion injury in rats. In our study, we found that the inhibitor couldn't cause neurological deficits and had no significant effects on synaptic/dendritic plasticity of rats without MCAO. It can be explained that under physiological conditions, the caveolin1/VEGF pathway is in an inactive state and the inhibitor does not work. In contrast, when cerebral ischemia-reperfusion occurs, the caveolin1/VEGF pathway is activated, and inhibitors can have a destructive effect on aggravating neurological deficits and increasing cerebral infarction volume by inhibiting the activated caveolin1/VEGF pathway. As expected, we found that an inhibitor could decrease the dendritic length, complexity and spine density of basilar and apical dendrites after 7 and 28 days. However, the downstream signaling molecular mechanism of VEGF is complex. As previously reported, VEGF can regulate dendritic growth and synaptogenesis by regulating the VEGFR2, PI3/AKT, and MAPK /MEK signaling pathways (Rosenstein et al., 2003). It is intriguing to speculate that VEGF may affect the transcriptional regulation and translation of neuronal microtubular proteins and play a role in soma to dendritic growth and maturation (Rosenstein et al., 2003). In primary neuronal cultures, VEGF can directly improve neural outgrowth in the absence of angiogenic or astroglial activity (Rosenstein et al., 2003). However, VEGF also can indirectly promote dendritic plasticity and synapse formation by improving neurovascular regeneration. Therefore, our experiment can only demonstrate that the caveolin-1/VEGF signal pathway participates in dendritic growth and synapse formation after cerebral ischemia reperfusion, but it cannot determine whether the caveolin-1/VEGF pathway directly mediates or indirectly promotes dendritic plasticity through angiogenesis and neurogenesis.

We further analyzed the relationship between exercise-induced dendritic plasticity and the caveolin-1/VEGF signaling pathway. As expected, the inhibitor suppressed the effects of exercise after MCAO. Compared with the EM7 group, a significantly shorter total dendritic length and lower spine density were observed for both basilar and apical dendrites in the IEM7 groups, consistent with the lower expression levels of caveolin-1 and VEGF. These results demonstrated that treadmill training promoted dendritic growth and dendritic spine formation through the caveolin-1/VEGF signaling pathway. Notably, there was no significant difference in the level of VEGF between the EM28 and IEM28 groups, indicating that caveolin-1/VEGF signaling played a necessary but not major role in exercise-mediated dendritic plasticity after 28 days and that other signaling molecules (e.g., BDNF, BFGF and Notch) might be involved in this process. Interestingly, compared with the EM7 group, the expression of caveolin-1 and VEGF was significantly decreased in the EM28 group, but the number of dendritic spines and total length and branches of dendrites were markedly increased. Intriguingly, growing evidence suggests that the molecular–genetic programs responsible for vessel formation can also influence neurite development and outgrowth, thereby raising the possibility that dendritic remodeling after stroke may be predicated on peri-infarct angiogenesis (Carmeliet and Tessier-Lavigne, 2005). Therefore, this result can be explained by the crucial role of early angiogenesis and neurogenesis mediated by the treadmill exercise-upregulated caveolin-1/VEGF signaling pathway in nutrition and support in the later stage. In addition, new neurons differentiate into mature neurons in 28 days, which may increase dendritic plasticity and synaptogenesis. Based on these results, we can reasonably speculate that the caveolin-1/VEGF signaling pathway may directly promote dendritic plasticity by affecting the transcriptional regulation and translation of neuronal microtubular proteins in the early recovery stage, whereas this pathway promotes dendrite plasticity indirectly by modulating angiogenesis and neurogenesis in the later stage. However, this hypothesis requires further analysis in vitro.

The major limitations of this study should be noted. First, due to the limitations of the experimental conditions, this experiment failed to use real-time detection of cerebral blood flow technology to unify the modeling, potentially leading to an instability of modeling complex cerebrovascular differences in rats. Second, dendrites, dendritic spines and synaptic changes were observed at morphological levels. Due to the limitations of the experimental conditions, no electrophysiological methods were used to detect the change in LTP at the functional level. Third, there were fewer signaling pathway proteins, and no in vitro experiments were performed. It was not clear whether the treadmill exercise-upregulated caveolin-1/VEGF pathway had direct or indirect effects on dendrites, spines and synapses. In view of the deficiencies of the experimental design, we will try our best to improve the experimental design in future experiments.

5. Conclusions

The findings of this study indicate that treadmill exercise plays a novel role in promoting dendritic and synaptic plasticity in the penumbra. Furthermore, the caveolin-1/VEGF signaling pathway can not only mediate dendritic and synaptic plasticity but is also involved in exercise-mediated dendritic and synaptic plasticity. However, treadmill-induced dendritic and synaptic plasticity after ischemic stroke is a complex, a cascade of signaling events and multi-channel process that involves many key factors and remains to be fully elucidated.

Author disclosure statement

No competing financial interests exist.

Acknowledgements

This study was supported by the Science Technology Bureau of Wenzhou funded project (No. 2017Y0961). We also appreciate the great technical assistance provided by the Experimental Animal Center of Wenzhou Medical University and the Laboratory Center of the Second Affiliated Hospital of Wenzhou Medical University & Yuying Children's Hospital.

References

Aoki, C., Miko, I., Oviedo, H., Mikeladze-Dvali, T., Alexandre, L., Sweeney, N., Bredt, D.S.,

2001. Electron microscopic immunocytochemical detection of PSD-95, PSD-93, SAP-102, and SAP-97 at postsynaptic, presynaptic, and nonsynaptic sites of adult and neonatal rat visual cortex. Synapse (New York NY) 40, 239–257.
Ashwal, S., Tone, B., Tian, H.R., Cole, D.J., Pearce, W.J., 1998. Core and penumbral nitric oxide synthase activity during cerebral ischemia and reperfusion. Stroke 29, 1037–1046 (discussion 1047).
Astrup, J., Siesjo, B.K., Symon, L., 1981. Thresholds in cerebral ischemia - the ischemic penumbra. Stroke 12, 723–725.
Benjamin, E.J, Virani, S.S., Callaway, C.W., Chamberlain, A.M., Chang, A.R., Cheng, S., Chiuve, S.E., Cushman, M., Delling, F.N., Deo, R., de Ferranti, S.D., Ferguson, J.F., Fornage, M., Gillespie, C., Isasi, C.R., Jimenez, M.C., Jordan, L.C., Judd, S.E., Lackland, D., Lichtman, J.H., Lisabeth, L., Liu, S., Longenecker, C.T., Lutsey, P.L., Mackey, J.S., Matchar, D.B., Matsushita, K., Mussolino, M.E., Nasir, K., O'Flaherty, M., Palaniappan, L.P., Pandey, A., Pandey, D.K., Reeves, M.J., Ritchey, M.D., Rodriguez, C.J., Roth, G.A., Rosamond, W.D., Sampson, U.K.A., Satou, G.M., Shah, S.H., Spartano, N.L., Tirschwell, D.L., Tsao, C.W., Voeks, J.H., Willey, J.Z., Wilkins, J.T., Wu, J.H., Alger, H.M., Wong, S.S., Muntner, P., 2018. Heart disease and stroke statistics-2018 update: a report from the American heart association. Circulation 137, e67–e492.
Benoist, M., Gaillard, S., Castets, F., 2006. The striatin family: a new signaling platform in dendritic spines. J. Physiol. Paris 99, 146–153.
Blizzard, C.A., Chuckowree, J.A., King, A.E., Hosie, K.A., McCormack, G.H., Chapman, J.A., Vickers, J.C., Dickson, T.C., 2011. Focal damage to the adult rat neocortex induces wound healing accompanied by axonal sprouting and dendritic structural plasticity. Cerebral cortex (New York NY) 1991 (21), 281–291.
Braun, J.E., Madison, D.V., 2000. A novel SNAP25-caveolin complex correlates with the onset of persistent synaptic potentiation. J. Neurosci. 20, 5997–6006.
Brown, C.E., Murphy, T.H., 2008. Livin' on the edge: imaging dendritic spine turnover in the peri-infarct zone during ischemic stroke and recovery. Neuroscientist 14, 139–146.
Brown, C.E., Li, P., Boyd, J.D., Delaney, K.R., Murphy, T.H., 2007. Extensive turnover of dendritic spines and vascular remodeling in cortical tissues recovering from stroke. J. Neurosci. 27, 4101–4109.
Budantsev, A., Kisliuk, O.S., Shul'govskii, V.V., Rykunov, D.S., Iarkov, A.V., 1993. The brain in stereotaxic coordinates (a textbook for colleges). Zh. Vyssh. Nerv. Deiat. Im. I. P. Pavlova 43, 1045–1051.
Carmeliet, P., Tessier-Lavigne, M., 2005. Common mechanisms of nerve and blood vessel wiring. Nature 436, 193–200.
Carmichael, S.T., 2003. Plasticity of cortical projections after stroke. Neuroscientist 9, 64–75.
Chen, J., Li, Y., Wang, L., Zhang, Z., Lu, D., Lu, M., Chopp, M., 2001. Therapeutic benefit of intravenous administration of bone marrow stromal cells after cerebral ischemia in rats. Stroke 32, 1005–1011.
Chen, K., Zhang, L., Tan, M., Lai, C.S., Li, A., Ren, C., So, K.F., 2017. Treadmill exercise suppressed stress-induced dendritic spine elimination in mouse barrel cortex and improved working memory via BDNF/TrkB pathway. Transl. Psychiatry 7, e1069.
Collaco-Moraes, Y., Aspey, B.S., de Belleroche, J.S., Harrison, M.J., 1994. Focal ischemia causes an extensive induction of immediate early genes that are sensitive to MK-801. Stroke 25, 1855–1860 (discussion 1861).
Corbett, D., Giles, T., Evans, S., McLean, J., Biernaskie, J., 2006. Dynamic changes in CA1 dendritic spines associated with ischemic tolerance. Exp. Neurol. 202, 133–138.
Dirnagl, U., Iadecola, C., Moskowitz, M.A., 1999. Pathobiology of ischaemic stroke: an integrated view. Trends Neurosci. 22, 391–397.
Fu, M., Yu, X., Lu, J., Zuo, Y., 2012. Repetitive motor learning induces coordinated formation of clustered dendritic spines in vivo. Nature 483, 92–95.
Gaillard, S., Bartoli, M., Castets, F., Monneron, A., 2001. Striatin, a calmodulin-dependent scaffolding protein, directly binds caveolin-1. FEBS Lett. 508, 49–52.
Gao, Y., Zhao, Y., Pan, J., Yang, L., Huang, T., Feng, X., Li, C., Liang, S., Zhou, D., Liu, C., Tu, F., Tao, C., Chen, X., 2014. Treadmill exercise promotes angiogenesis in the ischemic penumbra of rat brains through caveolin-1/VEGF signaling pathways. Brain Res. 1585, 83–90.
Garcia, P.C., Real, C.C., Ferreira, A.F., Alouche, S.R., Britto, L.R., Pires, R.S., 2012. Different protocols of physical exercise produce different effects on synaptic and structural proteins in motor areas of the rat brain. Brain Res. 1456, 36–48.
Gonzalez, C.L., Kolb, B., 2003. A comparison of different models of stroke on behaviour and brain morphology. Eur. J. Neurosci. 18, 1950–1962.
Gonzalez, C.L., Gharbawie, O.A., Williams, P.T., Kleim, J.A., Kolb, B., Whishaw, I.Q., 2004. Evidence for bilateral control of skilled movements: ipsilateral skilled forelimb reaching deficits and functional recovery in rats follow motor cortex and lateral frontal cortex lesions. Eur. J. Neurosci. 20, 3442–3452.
Harris, K.M., Kater, S.B., 1994. Dendritic spines: cellular specializations imparting both stability and flexibility to synaptic function. Annu. Rev. Neurosci. 17, 341–371.
Head, B.P., Hu, Y., Finley, J.C., Saldana, M.D., Bonds, J.A., Miyanohara, A., Niesman, I.R., Ali, S.S., Murray, F., Insel, P.A., Roth, D.M., Patel, H.H., Patel, P.M., 2011. Neuron-targeted caveolin-1 protein enhances signaling and promotes arborization of primary neurons. J. Biol. Chem. 286, 33310–33321.
Hickmott, P.W., Ethell, I.M., 2006. Dendritic plasticity in the adult neocortex. Neuroscientist 12, 16–28.
Huang, Y.F., Yang, C.H., Huang, C.C., Hsu, K.S., 2012. Vascular endothelial growth factor-dependent spinogenesis underlies antidepressant-like effects of enriched environment. J. Biol. Chem. 287, 40938–40955.
Hurtado, O., Cardenas, A., Pradillo, J.M., Morales, J.R., Ortego, F., Sobrino, T., Castillo, J., Moro, M.A., Lizasoain, I., 2007. A chronic treatment with CDP-choline improves functional recovery and increases neuronal plasticity after experimental stroke. Neurobiol. Dis. 26, 105–111.
Ito, U., Kuroiwa, T., Nagasao, J., Kawakami, E., Oyanagi, K., 2006. Temporal profiles of axon terminals, synapses and spines in the ischemic penumbra of the cerebral cortex: ultrastructure of neuronal remodeling. Stroke 37, 2134–2139.
Jiang, T., Xu, R.X., Zhang, A.W., Di, W., Xiao, Z.J., Miao, J.Y., Luo, N., Fang, Y.N., 2012. Effects of transcranial direct current stimulation on hemichannel pannexin-1 and neural plasticity in rat model of cerebral infarction. Neuroscience 226, 421–426.
Knott, G.W., Holtmaat, A., Wilbrecht, L., Welker, E., Svoboda, K., 2006. Spine growth precedes synapse formation in the adult neocortex in vivo. Nat. Neurosci. 9, 1117–1124.
Kolb, B., Brown, R., Witt-Lajeunesse, A., Gibb, R., 2001. Neural compensations after lesion of the cerebral cortex. Neural Plasticity 8, 1–16.
Li, Y., Jiang, N., Powers, C., Chopp, M., 1998. Neuronal damage and plasticity identified by microtubule-associated protein 2, growth-associated protein 43, and cyclin D1 immunoreactivity after focal cerebral ischemia in rats. Stroke 29, 1972–1980 (discussion 1980-1971).
Li, Y., Xu, X.L., Zhao, D., Pan, L.N., Huang, C.W., Guo, L.J., Lu, Q., Wang, J., 2015. TLR3 ligand Poly IC Attenuates Reactive Astrogliosis and Improves Recovery of Rats after Focal Cerebral Ischemia. CNS Neurosci. Therapeutics 21, 905–913.
Licht, T., Eavri, R., Goshen, I., Shlomai, Y., Mizrahi, A., Keshet, E., 2010. VEGF is required for dendritogenesis of newly born olfactory bulb interneurons. Development (Cambridge, England) 137, 261–271.
Lo, E.H., 2008. A new penumbra: transitioning from injury into repair after stroke. Nat. Med. 14, 497–500.
Mandyam, C.D., Schilling, J.M., Cui, W., Egawa, J., Niesman, I.R., Kellerhals, S.E., Staples, M.C., Busija, A.R., Risbrough, V.B., Posadas, E., Grogman, G.C., Chang, J.W., Roth, D.M., Patel, P.M., Patel, H.H., Head, B.P., 2017. Neuron-Targeted Caveolin-1 Improves Molecular Signaling, Plasticity, and Behavior Dependent on the Hippocampus in Adult and Aged mice. Biol. Psychiatry 81, 101–110.
Mostany, R., Portera-Cailliau, C., 2011. Absence of large-scale dendritic plasticity of layer 5 pyramidal neurons in peri-infarct cortex. J. Neurosci. 31, 1734–1738.
Nagerl, U.V., Kostinger, G., Anderson, J.C., Martin, K.A., Bonhoeffer, T., 2007. Protracted synaptogenesis after activity-dependent spinogenesis in hippocampal neurons. J. Neurosci. 27, 8149–8156.
Pang, Q., Zhang, H., Chen, Z., Wu, Y., Bai, M., Liu, Y., Zhao, Y., Tu, F., Liu, C., Chen, X., 2017. Role of caveolin-1/vascular endothelial growth factor pathway in basic fibroblast growth factor-induced angiogenesis and neurogenesis after treadmill training following focal cerebral ischemia in rats. Brain Res. 1663, 9–19.
Petralia, R.S., Wang, Y.X., Wenthold, R.J., 2003. Internalization at glutamatergic synapses during development. Eur. J. Neurosci. 18, 3207–3217.
Rosenstein, J.M., Mani, N., Khaibullina, A., Krum, J.M., 2003. Neurotrophic effects of vascular endothelial growth factor on organotypic cortical explants and primary cortical neurons. J. Neurosci. 23, 11036–11044.
Saver, J.L., Albers, G.W., Dunn, B., Johnston, K.C., Fisher, M., 2009. Stroke therapy academic industry roundtable (STAIR) recommendations for extended window acute stroke therapy trials. Stroke 40, 2594–2600.
Shih, P.C., Yang, Y.R., Wang, R.Y., 2013. Effects of exercise intensity on spatial memory performance and hippocampal synaptic plasticity in transient brain ischemic rats. PLoS ONE 8, e78163.
Shin, M.S., Jeong, H.Y., An, D.I., Lee, H.Y., Sung, Y.H., 2016. Treadmill exercise facilitates synaptic plasticity on dopaminergic neurons and fibers in the mouse model with Parkinson's disease. Neurosci. Lett. 621, 28–33.
Sholl, D.A., 1953. Dendritic organization in the neurons of the visual and motor cortices of the cat. J. Anat. 87, 387–406.
Swanson, R.A., Morton, M.T., Tsao-Wu, G., Savalos, R.A., Davidson, C., Sharp, F.R., 1990. A semiautomated method for measuring brain infarct volume. J. Cereb. Blood Flow Metab. 10, 290–293.
Toy, W.A., Petzinger, G.M., Leyshon, B.J., Akopian, G.K., Walsh, J.P., Hoffman, M.V., Vuckovic, M.G., Jakowec, M.W., 2014. Treadmill exercise reverses dendritic spine loss in direct and indirect striatal medium spiny neurons in the 1-methyl-4-phenyl-1,2,3,6-tetrahydropyridine (MPTP) mouse model of Parkinson's disease. Neurobiol. Dis. 63, 201–209.
Wiedenmann, B., Franke, W.W., 1985. Identification and localization of synaptophysin, an integral membrane glycoprotein of Mr 38,000 characteristic of presynaptic vesicles. Cell 41, 1017–1028.
Xu, T., Yu, X., Perlik, A.J., Tobin, W.F., Zweig, J.A., Tennant, K., Jones, T., Zuo, Y., 2009. Rapid formation and selective stabilization of synapses for enduring motor memories. Nature 462, 915–919.
Zhang, L., Hu, X., Luo, J., Li, L., Chen, X., Huang, R., Pei, Z., 2013. Physical exercise improves functional recovery through mitigation of autophagy, attenuation of apoptosis and enhancement of neurogenesis after MCAO in rats. BMC Neurosci. 14, 46.
Zhao, Y., Pang, Q., Liu, M., Pan, J., Xiang, B., Huang, T., Tu, F., Liu, C., Chen, X., 2017. Treadmill Exercise Promotes Neurogenesis in Ischemic Rat Brains via Caveolin-1/VEGF Signaling Pathways. Neurochem. Res. 42, 389–397.
Ziv, N.E., Smith, S.J., 1996. Evidence for a role of dendritic filopodia in synaptogenesis and spine formation. Neuron 17, 91–102.